J. Fluid Mech. (1995), *vol.* 293, *pp.* 349–378

The spreading of insoluble surfactant at the free surface of a deep fluid layer

By O. E. JENSEN

Department of Mathematics and Statistics, University of Newcastle upon Tyne, Newcastle upon Tyne NE1 7RU, UK

(Received 25 August 1994 and in revised form 25 February 1995)

The unsteady spreading of an insoluble monolayer containing a fixed mass of surface-active material over the initially horizontal free surface of a viscous fluid layer is investigated. A flow driving the spreading is induced by gradients in surface tension, which arise from the nonuniform surfactant distribution. Distinct phases in the flow's dynamics are distinguished by a time $T = H_0^2/\nu$, where H_0 is the fluid depth and ν its viscosity. For times $t \ll T$, i.e. before the lower boundary has any significant influence on the flow, a laminar sub-surface boundary-layer flow is generated. The effects of gravity, capillarity, surface diffusion or surface contamination may be weak enough for the flow to drive a substantial unsteady displacement of the free surface, upward behind the monolayer's leading edge and downward towards its centre. Similarity solutions are identified describing the spreading of a localized planar monolayer strip (which spreads like $t^{1/2}$) or an axisymmetric drop (which spreads like $t^{3/8}$); using the Prandtl transformation, the associated boundary-layer problems are solved numerically. Quasi-steady sub-layers are shown to exist at the centre and at the leading edge of the monolayer; that due to surface contamination, for example, may eventually grow to dominate the flow, in which case spreading proceeds like $t^{3/4}$. Once $t = O(T)$, vorticity created at the free surface has diffused down to the lower boundary and the flow changes character, slowing appreciably. The dynamics of this stage are modelled by reducing the problem to a single nonlinear diffusion equation. For a spreading monolayer strip or drop, the transition from an inertia-dominated (boundary-layer) flow to a viscosity-dominated (thin-film) flow is predicted to be largely complete once $t \approx 85T$.

1. Introduction

The spreading of surface-active material over the free surface of a viscous fluid layer through the action of surface-tension gradients may occur in widespread contexts. During the later stages of the spreading of an oil slick on the sea, for example, the oil forms an ultra-thin layer (a monolayer), the thickness of which determines the local surface tension; a gradient in surface tension is distributed across the length of the slick, and this stress induces a viscous flow in the fluid beneath, which drives the spreading of the oil (Hoult 1972; DiPietro, Huh & Cox 1978). Alternatively, the surface-active material may be a surfactant which adsorbs at the fluid's free surface to form a monomolecular layer; the surface tension is then inversely related to the local surface concentration of surfactant. Thus a monolayer, be it an organic surfactant, a film-forming organic liquid, or an aqueous surfactant solution on an oil phase (Joos & van Hunsel 1985), will spread spontaneously until concentration

gradients are eliminated. Monolayer spreading has long been of central importance in surface chemistry (see, for example, Karkare, La & Fort 1993) and such flows also have important applications in industrial and biological contexts, where frequently the substrate fluid is very thin. Much fluid-dynamical work in recent years has been motivated by interest in the role played by surfactant in lung mechanics, for example (Grotberg 1994).

Theoretical investigations of monolayer spreading have concentrated predominantly on insoluble surfactants, and the majority are long-wavelength approximations, i.e. it is assumed that the longitudinal lengthscale of variation of the monolayer greatly exceeds the characteristic depth of the flow (where this depth is the typical distance over which vorticity, created by shear stresses at the free surface, penetrates by the action of viscosity). Such studies fall into two distinct classes: the 'thin-layer' theories, in which lubrication theory is used to derive a pair of coupled evolution equations for the flow; and the more complex 'deep-layer' theories, in which the surfactant transport equation is coupled to an unsteady viscous boundary-layer flow. Two features of both classes are worth emphasizing. The first is that, in general, the fluid velocities parallel to the free surface are spatially nonuniform. For thin fluid layers, the fluid's incompressibility therefore demands that there is deformation of the free surface, so that typically the fluid surface is elevated towards the front of the advancing monolayer, and depressed upstream of this (Borgas & Grotberg 1988; Gaver & Grotberg 1990; Troian, Herbolzheimer & Safran 1990). The possibility of surface deformation in deep-layer flows, arising through this mechanism, will be considered below. The second important feature of both the thin-layer and deep-layer cases is that unsteady flows, in which there is a dominant balance between viscous forces and surface-tension gradients, are asymptotically self-similar at large times. In the thin-layer situation, for example, Jensen & Grotberg (1992, hereinafter referred to as JG) showed that a dilute planar monolayer strip, containing a fixed mass of surfactant, spreads like $t^{1/3}$ (see also Espinosa *et al.* 1993), an axisymmetric monolayer drop, also of fixed mass, spreads like $t^{1/4}$ (confirming the numerical predictions of Gaver & Grotberg 1990), while a monolayer spreading from a line or point source of constant surfactant concentration (which we call here a planar or axisymmetric 'front') spreads like $t^{1/2}$ (consistent with Ahmad & Hansen 1972). The deep-layer analogue of the planar front solution was determined by Foda & Cox (1980), who showed that a monolayer fed from a source of constant concentration spreads like $t^{3/4}$ (see also Hoult 1972; Joos & Pintens 1977). The aim of the present paper is to describe two important cases of the deep-layer problem that have not yet been investigated, namely the spreading of a planar monolayer strip or an axisymmetric drop, and to provide a simple account of how, in the presence of a solid boundary beneath the fluid layer, these flows evolve at large times into the corresponding thin-layer flows described in JG. The effects on these deep-layer flows of surface contamination by low levels of pre-existing surfactant, which is likely to be important both experimentally and in practical applications, will also be considered.

The appropriate scalings for the deep-layer flows are readily determined, as follows. Suppose a spreading, insoluble monolayer is localized, having length $L(t)$ at time t and that the total mass of surfactant (or oil) is M. Let the underlying fluid have constant density ρ and constant viscosity μ. For simplicity, we assume that the monolayer is sufficiently dilute for physico-chemical nonlinearities in the relation between surface tension σ and the surfactant's surface concentration Γ to be unimportant, so that surface activity is represented by a single parameter $A = -\mathrm{d}\sigma/\mathrm{d}\Gamma$ (> 0). Then, writing '$\sim$' for 'scales like', the horizontal coordinate $x \sim L$, the horizontal velocity

$u \sim L/t$, and $\Gamma \sim M/L^n$, say, where where $n = 0$ for a front, $n = 1$ for a strip and $n = 2$ for a drop. A horizontal momentum balance, $\rho u u_x \sim \mu u_{zz}$ (where subscripts denote derivatives), implies that the downward vertical coordinate $z \sim (\nu t)^{1/2}$, where $\nu = \mu/\rho$ (representing downward diffusion of vorticity), and then a tangential stress balance at the free surface, $\mu u_z \sim \sigma_x = -A\Gamma_x$, implies that

$$L \sim \left(\frac{A^2 M^2 t^3}{\rho\mu}\right)^{1/[2(n+2)]}. \tag{1.1}$$

Thus (1.1) recovers the $t^{3/4}$-scaling for a front, and shows also that a planar strip spreads like $t^{1/2}$ and an axisymmetric drop like $t^{3/8}$. The corresponding self-similar solutions for the two fixed-mass monolayer configurations of the unsteady, two-dimensional boundary-layer equations, allowing for surface deformation, are determined numerically in §3 below.

The first investigations of surfactant spreading over deep layers in which the fluid mechanics was treated fully considered the steady advance of a localized, insoluble monolayer against a uniform stream. In this case, the monolayer acts as a rigid plate along its length, and the flow beneath the monolayer is a Blasius boundary layer (Harper & Dixon 1974; DiPietro *et al.* 1978). The surfactant distribution necessary to support the viscous shear stress is therefore proportional to $x^{1/2}$, where x is the distance from the leading edge of the monolayer. This flow configuration was re-examined in the zero-Reynolds-number limit by Harper (1992). In unsteady spreading, however, the monolayer acts as a rigid plate only at its leading edge. Foda & Cox (1980) showed that for a spreading planar front, for example, the surfactant distribution has a Blasius structure locally, but they had to compute the boundary-layer flow numerically over the remainder of the monolayer, patching this to a further inner region near the stationary source of surfactant. They assumed that the length of this inner region grew at the same rate as the full monolayer, but found that the region was then sensitive to the form of the nonlinear equation of state chosen, a restriction that was reconsidered by Dagan (1984). It will be shown in §3.2 below that the fixed-mass solutions also have the local Blasius structure at the leading edge, where a range of singular effects may manifest themselves. The unsteady stretching flow at the midpoint of a strip or a drop may also exhibit a distinct inner region, if surface deformation is taken into account. Evidence will be presented in §3.1 suggesting that this inner region is *unsteady* relative to the spreading monolayer, and is instead steady in the laboratory frame.

There have been numerous reports of a slight rise in the free surface at the leading edge of an advancing monolayer on deep fluid, the so-called 'Reynolds ridge' (e.g. Mockros & Krone 1968; McCutchen 1970). The ridge was modelled by Harper & Dixon (1974), who examined the transition between a uniform flow state and a rigid monolayer. The advancing monolayer causes downward displacement of the oncoming fluid; this displacement generates a nonuniform pressure distribution beneath the leading-edge boundary layer through inertial effects. The free surface responds by adjusting its shape so that the pressure field can be supported by gravitational and surface tension forces. Harper & Dixon showed that there is an elevation of the free surface at the monolayer's leading edge, with a weaker depression beyond, predictions that were verified experimentally by Scott (1982).

With the exception of Harper & Dixon (1974), however, in all theoretical deep-layer studies it has been assumed that the free surface remains flat. Harper (1992) showed that this assumption is consistent with the surface boundary conditions for

a deep layer in steady Stokes flow. This is also a realistic assumption for large oil slicks, for example, for which gravity provides a strong restoring force. In this case, an irrotational flow with finite vertical velocity is induced beneath the boundary layer, such that fluid is displaced downwards beneath the advancing monolayer's rigid leading edge, and is drawn upwards beneath regions of the monolayer where there is longitudinal stretching of the free surface (e.g. figure 3*a*, below). For much smaller monolayers, however, the effects of gravity are substantially weaker, and in the absence of this or other restoring forces there is no mechanism for the generation of vertical motion beneath the boundary layer. Instead, it will be shown below that the nonuniform horizontal velocity may, via a mechanism quite distinct from that producing the Reynolds ridge, generate significant free-surface deformation (figure 3*b*, below), which grows (in the vertical direction) asymptotically like $(\nu t)^{1/2}$, while all disturbances to the fluid far beneath the monolayer are exponentially small. The Prandtl transformation of the unsteady boundary-layer equations is used (in §2) to show the direct correspondence between flows in which the free surface either remains flat or deforms freely.

The deep-layer scaling law (1.1) is valid provided the monolayer is spreading over a clean interface. Contamination of the interface by a weak, uniform distribution of surfactant of concentration Γ_∞, say, is a potentially common situation, however, and is of interest because it can significantly influence spreading rates. For example, the surfactant concentration at the midpoint of a spreading strip or drop diminishes like $t^{-1/2}$ or $t^{-3/4}$ respectively, and so will ultimately fall to a level comparable with the level of contamination. In this case, the boundary-layer equations may be linearized, as outlined in §4 below, where it is shown that the spreading flow is again self-similar, with

$$x \sim \left(\frac{S_\infty^2 t^3}{\rho\mu}\right)^{1/4} \tag{1.2}$$

for both the strip or the drop. In (1.2), $S_\infty = A\Gamma_\infty$ is the surface-tension difference between a clean and a contaminated interface. Flow disturbances now spread at a rate determined by the degree of contamination, although the distance travelled by the deposited monolayer remains dependent on its strength M (Grotberg, Halpern & Jensen 1995).

Finally, a heuristic model will be used to explore the link between the deep-layer and thin-layer results by considering the spreading of a monolayer over a fluid layer of finite depth. A simple approximation is used to reduce both problems, and the intermediate finite-depth case, to a single nonlinear diffusion equation ((5.3) and (5.7) below). This is used to examine the transition between the high-Reynolds-number, boundary-layer flow, in which a monolayer strip, say, spreads like $t^{1/2}$, and the low-Reynolds-number thin-film flow, in which a strip spreads like $t^{1/3}$. In this simple model, spreading remains self-similar although the monolayer length $L(t)$ satisfies a nonlinear ordinary differential equation. It is shown how inertial effects are ultimately confined to a shrinking inner layer at the monolayer's leading edge.

2. The model for a monolayer spreading over deep fluid

Consider a monolayer lying on the initially horizontal free surface of a deep layer of fluid. Coordinates (x, z) are defined with x horizontal, z increasing downwards into the fluid and the free surface at $z = h(x, t)$; the corresponding velocity components are $u(x, z, t)$ and $w(x, z, t)$. Gravity g acts in the z-direction. The surfactant is assumed

dilute and insoluble, having constant surface diffusivity D. The surface tension of the interface when uncontaminated is σ_0.

To make the boundary-layer approximation, we introduce a horizontal lengthscale L_0, a vertical lengthscale ϵL_0 where $\epsilon \ll 1$, a velocity scale $U_0 = A\Gamma_0\epsilon/\mu$, where Γ_0 is a scale for the surfactant concentration and A is the surfactant activity, a Reynolds number $Re = \rho U_0 L_0/\mu$, a gravitational parameter $\mathscr{G} = \epsilon g L_0/U_0^2$, a diffusive parameter $\mathscr{D} = D/U_0 L_0$ (an inverse Péclet number) and a capillary parameter $\mathscr{S} = \epsilon\sigma_0/\rho U_0^2 L_0$. We let $\sigma = \sigma_0\hat{\sigma}(\Gamma)$, where $\Gamma = \Gamma(x,t)$. Since we are interested in the large-Reynolds-number limit, we set $Re = \mathscr{R}/\epsilon^2$, where $\mathscr{R} = O(1)$ or larger. Nondimensionalizing, by scaling x on L_0, z and h on ϵL_0, t on L_0/U_0, u on U_0, w on ϵU_0, Γ on Γ_0, and p on ρU_0^2, and neglecting terms that are $O(\epsilon^2)$ or smaller, the mass-conservation and Navier–Stokes equations reduce to the boundary-layer equations,

$$\partial_x u + w_z = 0, \tag{2.1}$$

$$u_t + uu_x + wu_z = -p_x + \mathscr{R}^{-1}u_{zz}, \tag{2.2}$$

$$0 = -p_z + \mathscr{G}, \tag{2.3}$$

where $\partial_x u \equiv u_x$ in a planar geometry and $\partial_x u \equiv x^{-1}(xu)_x$ in an axisymmetric geometry. The corresponding leading-order boundary conditions at the free surface $z = h(x,t)$, (where $u_s(x,t) \equiv u(x,h,t)$ etc.), are

$$h_t + u_s h_x = w_s, \qquad \Gamma_t + \partial_x(u_s\Gamma) = \mathscr{D}\partial_x\Gamma_x, \qquad u_z = \Gamma_x \tag{2.4}$$

and

$$p = \mathscr{S}\hat{\sigma}(\Gamma)h_{xx}. \tag{2.5}$$

These are respectively the kinematic condition, the surfactant transport equation, and the tangential and normal stress conditions. Appropriate boundary conditions at $z \to \infty$ are also required, and are given below. In addition the parameter M, representing either the total mass of surfactant in the monolayer, or the surfactant concentration at a source, has a nondimensional equivalent $\mathscr{M}$, where

$$M = \mathscr{M}\Gamma_0 L_0^n. \tag{2.6}$$

The cases of a spreading monolayer front, strip or drop correspond to $n = 0$, 1 or 2 respectively; intermediate values of n represent a range of source strengths.

Combining (2.3) and (2.5) gives the pressure in the boundary layer

$$p(x,z,t) = \mathscr{G}(z-h) + \mathscr{S}\hat{\sigma}(\Gamma)h_{xx},$$

and so (2.2) becomes

$$u_t + uu_x + wu_z = \mathscr{G}h_x - \mathscr{S}\{\hat{\sigma}(\Gamma)h_{xx}\}_x + \mathscr{R}^{-1}u_{zz}. \tag{2.7}$$

Deflection of the free surface from the horizontal generates a pressure field that is transmitted instantaneously through the boundary layer, driving an irrotational inviscid (outer) flow at depth. This flow couples back to the boundary-layer flow through the boundary condition $u \to u_e(x,t)$, say, as $z \to \infty$, where u_e is the solution of the outer problem evaluated at the free surface. We shall concentrate largely on cases in which such interactions are unimportant. Making such an assumption (justified more fully in §2.2 below), (2.7) reduces to

$$u_t + uu_x + wu_z = \mathscr{R}^{-1}u_{zz}. \tag{2.8}$$

In allowing the free surface to deform, we impose the condition (readily verified *a*

posteriori) that the vorticity generated at the free surface decays exponentially beneath the boundary layer (Goldstein 1965), and that there is no downward displacement of fluid beneath the boundary layer. The remaining boundary conditions for the simplified problem (2.1), (2.4) and (2.8) are therefore

$$u \to 0, \quad w \to 0 \quad \text{exponentially as } z \to \infty. \tag{2.9}$$

The kinematic condition in (2.4) is now equivalent to $h_t = \partial_x q$, where the flow rate $q(x,t) = \int_h^\infty u \, \mathrm{d}z$.

2.1. *Self-similar solutions*

Balancing terms in equations (2.1), (2.4) and (2.8) with $\mathscr{D} = 0$, following the scaling arguement used to derive (1.1), one finds that

$$x \sim \left(\mathscr{M}^2 t^3/\mathscr{R}\right)^{1/[2(n+2)]}, \qquad z \sim \left(t/\mathscr{R}\right)^{1/2}. \tag{2.10}$$

An important condition of self-consistency is that the boundary layer is thin, i.e. $z \ll x$. This condition is met for a front ($n = 0$), strip ($n = 1$) and drop ($n = 2$) provided

$$t \gg (\mathscr{R}\mathscr{M}^2)^{-1}, \qquad (\mathscr{R}\mathscr{M})^2 \gg 1, \qquad t \ll \mathscr{R}^3\mathscr{M}^2$$

respectively. For the typical parameter values given in §2.2 below, it is only at extremely large times for the drop flow that the boundary layer might grow too thick for the long-wavelength theory to be valid. In this case, because the flow is continually slowing, its effective Reynolds number (which is proportional to $LL_t \sim t^{-1/4}$) is continually diminishing, so that at sufficiently large times a Stokes flow can be anticipated: in this case, vorticity penetrates a depth of (at least) the order of the monolayer length (Lister & Kerr 1989), and repeating the scaling argument of §1 with $z \sim L$ implies that $L \sim (AMt/\mu)^{1/3}$, i.e. the spreading rate changes from $t^{3/8}$ to $t^{1/3}$.

We incorporate the scaling (2.10) by defining new independent variables

$$\xi = x\left(\mathscr{R}/\mathscr{M}^2 t^3\right)^{1/[2(n+2)]}, \quad \eta = z\left(\mathscr{R}/t\right)^{1/2}, \quad \tau = t$$

and new variables dependent on ξ, η and τ (chosen using the scaling arguments given in §1)

$$H = \left(\mathscr{R}/t\right)^{1/2} h, \quad Q = \left(\mathscr{R}t^{n-1}/\mathscr{M}^2\right)^{1/[2(n+2)]} q, \quad G = \left(t^{3n}/\mathscr{M}^4\mathscr{R}^n\right)^{1/[2(n+2)]} \Gamma,$$

$$U = \left(\mathscr{R}t^{2n+1}/\mathscr{M}^2\right)^{1/[2(n+2)]} u, \quad W = (\mathscr{R}t)^{1/2} w.$$

Then (2.1), (2.8), (2.4) (with $\mathscr{D} = 0$) and (2.9) become respectively

$$\partial_\xi U + W_\eta = 0, \tag{2.11}$$

$$\tau U_\tau + UU_\xi + WU_\eta = U_{\eta\eta} + \frac{3}{2(n+2)}\xi U_\xi + \tfrac{1}{2}\eta U_\eta + \frac{(2n+1)}{2(n+2)}U, \tag{2.12}$$

$$\left.\begin{aligned} \tau H_\tau + \tfrac{1}{2}H + \left(U_s - \frac{3}{2(n+2)}\xi\right)H_\xi &= W_s \\ \tau G_\tau - \frac{3}{2(n+2)}(nG + \xi G_\xi) + \partial_\xi(U_s G) &= 0 \\ U_\eta &= G_\xi \end{aligned}\right\} \quad \text{on } \eta = H(\xi,\tau),$$

$$U \to 0, \quad W \to 0 \quad \text{exponentially as } \eta \to \infty.$$

The kinematic condition can be written in terms of the transformed flow rate Q as

$$\tau H_\tau + \tfrac{1}{2}H - \frac{3}{2(n+2)}\xi H_\xi = \partial_\xi Q \qquad \text{where} \quad Q(\xi,\tau) = \int_{H(\xi,\tau)}^{\infty} U(\xi,\eta,\tau)\,\mathrm{d}\eta. \tag{2.13}$$

We shall later seek solutions that are independent of τ, but it is helpful to retain the time-dependent terms at this stage.

2.2. *Diffusion, gravity and capillarity*

Before proceeding further, it is important to establish the importance of these three effects, so that we know the conditions under which each may be justifiably neglected. We therefore return briefly to the full boundary-layer equation (2.7) and the surfactant transport equation in (2.4), and re-write them in transformed variables, giving respectively

$$\tau U_\tau + UU_\xi + WU_\eta = U_{\eta\eta} + \frac{3}{2(n+2)}\xi U_\xi + \tfrac{1}{2}\eta U_\eta + \frac{(2n+1)}{2(n+2)}U + \hat{\mathscr{G}}H_\xi - \hat{\mathscr{S}}H_{\xi\xi\xi},$$

$$\tau G_\tau - \frac{3}{2(n+2)}(nG + \xi G_\xi) + \partial_\xi(U_s G) = \hat{\mathscr{D}}\partial_\xi G_\xi.$$

(For convenience we have set $\hat{\sigma}(\Gamma) = \hat{\sigma}(0) = 1$.) Diffusivity, gravity and capillarity are now represented by the time-dependent quantities

$$\hat{\mathscr{D}} = \mathscr{D}t^{(n-1)/(n+2)}, \quad \hat{\mathscr{G}} = \mathscr{G}\left(\frac{t^{5n+4}}{\mathscr{M}^4\mathscr{R}^n}\right)^{1/[2(n+2)]} \quad \text{and} \quad \hat{\mathscr{S}} = \mathscr{S}\left(\frac{\mathscr{R}^{2-n}t^{5n-2}}{\mathscr{M}^8}\right)^{1/[2(n+2)]}. \tag{2.14}$$

Each of $\hat{\mathscr{D}}$, $\hat{\mathscr{G}}$ and $\hat{\mathscr{S}}$ must remain small for the corresponding forces have a weak effect relative to the basic flow or to be confined to narrow regions of the flow. These three effects become significant at times $T_{\mathscr{D}}$, $T_{\mathscr{G}}$ and $T_{\mathscr{S}}$, when $\hat{\mathscr{D}}$, $\hat{\mathscr{G}}$ and $\hat{\mathscr{S}}$ are each $O(1)$. These timescales are given in table 1, along with conditions for each to be large; it is then straightforward to determine which of the three timescales is the smallest for a particular flow.

Table 1 can be used to predict the sequence of events. For a front, diffusive and capillary effects both diminish relative to the strength of the flow (because $\hat{\mathscr{D}}$ and $\hat{\mathscr{S}}$ are diminishing functions of time with $n = 0$), and so can be expected to be confined to shrinking boundary layers at the monolayer's leading edge (see §3.2 below); gravity will ultimately dominate at a time of $O(T_{\mathscr{G}})$. For a strip, either gravity or capillarity will be the first to dominate at large times, although gravity will always dominate ultimately. The effects of diffusion are steady in the frame of the spreading strip. For the slower-spreading drop, any of the three effects may be the first to dominate, depending on a delicate balance of parameters, although gravity will again dominate ultimately.

Parameter values appropriate for a typical surfactant spreading on water are as follows, to the nearest order of magnitude: $g \approx 10^3$ cm s^{-2}; $\rho \approx 1$ g cm^{-3}; $\mu \approx 10^{-2}$ cm^{-1}s^{-1}; $\sigma \approx 100$ g s^{-2}; $A\Gamma_0 \approx 10$ g s^{-2}; $D \approx 10^{-5}$ cm^{2}s^{-1}. If we assume $\epsilon \approx 10^{-1}$, $L_0 \approx 1$ cm, then $U_0 \approx 10^2$ cm s^{-1} and $Re \approx 10^4$. (At such large Reynolds numbers the flow may experience instabilities, at least early during spreading, but these are beyond the scope of the present study.) The nondimensional parameters then take the following values: $\mathscr{R} \approx 100$; $\mathscr{G} \approx 10^{-2}$; $\mathscr{S} \approx 10^{-3}$; $\mathscr{D} \approx 10^{-7}$ and $\mathscr{M} \approx 1$. Thus, even for a relatively large monolayer, with $L \approx 1$ cm, gravity is weak. For much

	Front	Strip	Drop
$T_{\mathscr{D}}$	$\mathscr{D}^2$	–	$\mathscr{D}^{-4}$
$T_{\mathscr{G}}$	$\mathscr{M}/\mathscr{G}$	$(\mathscr{M}^4\mathscr{R}/\mathscr{G}^6)^{1/9}$	$(\mathscr{M}^2\mathscr{R}/\mathscr{G}^4)^{1/7}$
$T_{\mathscr{S}}$	$\mathscr{S}^2\mathscr{R}/\mathscr{M}^4$	$(\mathscr{M}^8/\mathscr{S}^6\mathscr{R})^{1/3}$	$\mathscr{M}/\mathscr{S}$
$T_{\mathscr{D}} \gg 1$	–	$\mathscr{D} \ll 1$	$\mathscr{D} \ll 1$
$T_{\mathscr{G}} \gg 1$	$\mathscr{G} \ll \mathscr{M}$	$\mathscr{G} \ll (\mathscr{M}^4\mathscr{R})^{1/6}$	$\mathscr{G} \ll (\mathscr{M}^2\mathscr{R})^{1/4}$
$T_{\mathscr{S}} \gg 1$	–	$\mathscr{S} \ll (\mathscr{M}^8/\mathscr{R})^{1/6}$	$\mathscr{S} \ll \mathscr{M}$

TABLE 1. Timescales for diffusion, gravity and capillarity to significantly influence the flow.

smaller monolayers, gravity becomes even weaker, while diffusion and capillarity are relatively more significant. For $\mathscr{R}$ to be $O(1)$ or larger we need $L \gg 10^{-2}$ cm, which guarantees that $\mathscr{D} \ll \mathscr{S} \ll 1$; for $\mathscr{G} \ll 1$ we need $L \ll 100$ cm. Our theory allowing for free-surface deformation is therefore appropriate for 10^{-2} cm $\ll L \ll 10^2$ cm (over appropriate time intervals, of course).

2.3. *Prandtl transformation*

We now return to the basic flow of §2.1, neglecting gravitational, diffusive or capillary effects. Restricting attention for the present to a planar geometry, we can introduce a stream function $\psi(\xi,\eta,\tau)$, where $U = \psi_\eta$, $W = -\psi_\xi$ to satisfy (2.11) automatically. Then (2.12) becomes

$$\tau\psi_{\eta\tau} + \psi_\eta\psi_{\xi\eta} - \psi_\xi\psi_{\eta\eta} = \psi_{\eta\eta\eta} + \frac{3}{2(n+2)}\xi\psi_{\xi\eta} + \tfrac{1}{2}\eta\psi_{\eta\eta} + \frac{(2n+1)}{2(n+2)}\psi_\eta, \tag{2.15}$$

supplemented by the boundary conditions

$$\left.\begin{aligned} \tau H_\tau + \tfrac{1}{2}H + \left(\psi_\eta - \frac{3}{2(n+2)}\xi\right)H_\xi &= -\psi_\xi \\ \tau G_\tau - \frac{3}{2(n+2)}(nG + \xi G_\xi) + \left[(\psi_\eta)_s G\right]_\xi &= 0 \\ \psi_{\eta\eta} &= G_\xi \end{aligned}\right\} \quad \text{on } \eta = H(\xi,\tau), \tag{2.16}$$

$$\psi \to 0 \quad \text{exponentially as } \eta \to \infty. \tag{2.17}$$

Note also that $Q(\xi,\tau) = -\psi(\xi,H,\tau)$, so that the kinematic condition can be written $\tau H_\tau + \frac{1}{2}(H - [3/(n+2)]\xi H_\xi) = (-\psi(\xi,H,\tau))_\xi$.

This set of equations can be converted from a free-boundary to a fixed-boundary problem via the Prandtl transformation, a symmetry of the unsteady boundary-layer equations (Ma & Hui 1990), by defining new variables $X = \xi$, $Y = \eta - H(\xi,\tau)$, $T = \tau$ and introducing a new stream function

$$\Phi(X,Y,T) = \psi(\xi,\eta,\tau) + \int_\infty^X \left\{\tau H_\tau + \tfrac{1}{2}\left(H - \frac{3}{(n+2)}\xi H_\xi\right)\right\} \mathrm{d}\xi \equiv \psi(\xi,\eta,\tau) - \psi(\xi,H,\tau). \tag{2.18}$$

This choice of integral ensures that $\Phi \to 0$ as $X \to \infty$, i.e. far ahead of the monolayer the fluid is undisturbed. Under this transformation (2.15) is invariant, i.e.

$$T\Phi_T + \Phi_Y\Phi_{XY} - \Phi_X\Phi_{YY} = \Phi_{YYY} + \frac{3}{2(n+2)}X\Phi_{XY} + \tfrac{1}{2}Y\Phi_{YY} + \frac{(2n+1)}{2(n+2)}\Phi_Y. \tag{2.19}$$

The kinematic boundary condition becomes $\Phi_X(X,0) = 0$, which we can therefore replace by $\Phi(X,0) = 0$. Thus the boundary conditions (2.16) and (2.17) become

$$\left.\begin{aligned} \Phi &= 0 \\ TG_T - \frac{3}{2(n+2)}(nG + XG_X) + [\Phi_Y G]_X &= 0 \\ \Phi_{YY} &= G_X \end{aligned}\right\} \quad \text{on } Y = 0, \tag{2.20}$$

$$\Phi \to Q(X,T) = \int_{\infty}^{X} \left\{ TH_T + \tfrac{1}{2}\left(H - \frac{3}{(n+2)}\xi H_\xi\right)\right\} \mathrm{d}\xi \quad \text{exponentially as } Y \to \infty. \tag{2.21}$$

Thus the original problem (2.15)–(2.17), for which the free surface deforms while the flow generates no vertical displacement of fluid beneath the boundary layer, is completely equivalent to the transformed problem (2.19)–(2.21) in which the free surface is constrained (for example by gravity) to remain flat.

A similar formulation can be undertaken for an axisymmetric geometry. In this case, the stream function $\psi(\xi,\eta,\tau)$ is defined by $U = \psi_\eta/\xi$, $W = -\psi_\xi/\xi$. Again, the Prandtl transformation may be employed, defining $X = x$, $Y = \eta - H(\xi,\tau)$, $T = \tau$ and

$$\Phi(X,Y,T) = \psi(\xi,\eta,\tau) + \int_{\infty}^{X} \xi\left(TH_T + \tfrac{1}{2}H - \frac{3}{2(n+2)}\xi H_\xi\right)\mathrm{d}\xi \equiv \psi(\xi,\eta,\tau) - \psi(\xi,H,\tau).$$

The momentum equation is now

$$T\Phi_T + \frac{1}{X}(\Phi_Y\Phi_{XY} - \Phi_X\Phi_{YY}) - \frac{\Phi_Y^2}{X^2} = \Phi_{YYY} + \frac{3}{2(n+2)}X\Phi_{XY} + \tfrac{1}{2}Y\Phi_{YY} + \left(\frac{n-1}{n+2}\right)\Phi_Y, \tag{2.22}$$

and the boundary conditions become

$$\left.\begin{aligned} \Phi &= 0 \\ TG_T - \frac{3}{2(n+2)}(nG + XG_X) + \frac{1}{X}[\Phi_Y G]_X &= 0 \\ \Phi_{YY} &= XG_X \end{aligned}\right\} \quad \text{on } Y = 0, \tag{2.23}$$

$$\Phi \to XQ(X,T) = \int_{\infty}^{X} \xi\left(TH_T + \tfrac{1}{2}H - \frac{3}{2(n+2)}\xi H_\xi\right)\mathrm{d}\xi \quad \text{exponentially as } Y \to \infty. \tag{2.24}$$

2.4. *Statement of the self-similar strip and drop problems*

Solutions of (2.19)–(2.21) or (2.22)–(2.24) that are independent of T are similarity solutions of the unsteady boundary-layer equations describing the spreading of an insoluble monolayer. The T-independent solution of (2.19)–(2.21) with $n = 0$ was essentially that computed by Foda & Cox (1980), for example. In §3 below we seek the complementary similarity solutions for a strip, i.e. (2.19)–(2.21) with $n = 1$, and for a drop, i.e. (2.22)–(2.24) with $n = 2$. These problems are simplified by the fact that in each case the surfactant distribution decouples from the flow. Assuming T-independence, the surfactant transport equations in (2.20) and (2.23) become

$$[(\Phi_Y - \tfrac{1}{2}X)G]_X = 0 \quad \text{(strip)}, \qquad [(\Phi_Y - \tfrac{3}{8}X^2)G]_X = 0 \quad \text{(drop)} \qquad \text{on } Y = 0.$$

Thus ahead of the monolayer, $G = 0$ and the fluid is completely undisturbed, while beneath the monolayer there is a linear stretching flow of finite extent with surface velocity $U_s = \frac{1}{2}X$ (strip) or $U_s = \frac{3}{8}X$ (drop), i.e. $u_s = [3/2(n+2)](x/t)$ in the original variables. This is very similar to the unsteady spreading of an oil slick, driven by a balance between a hydrostatic pressure force, arising from the nonuniform thickness of the slick, and viscous forces in the fluid beneath. In this case, after transformation into suitable similarity variables, Hoult (1972) showed that the oil continuity equation is satisfied by a velocity field of the form $u_s \propto (x/t)$. Hoult hypothesized that the leading edge of the advancing slick pushes fluid ahead of it, generating a region of reversed flow at depth; Buckmaster (1973) showed that this is not in fact the case, and that the flow is everywhere forward. Buckmaster's results (for a planar horizontal slick) carry over directly to the present problem.

We assume that the monolayer lies in $|X| \leqslant 1$. The strip problem is then as follows:

$$\Phi_Y \Phi_{XY} - \Phi_X \Phi_{YY} = \Phi_{YYY} + \tfrac{1}{2}[X\Phi_X + Y\Phi_Y]_Y\,; \tag{2.25}$$

$$\Phi = 0, \quad \Phi_Y = \tfrac{1}{2}X, \quad \Phi_{YY} = G_X \quad \text{on } Y = 0, \quad 0 \leqslant X \leqslant 1; \qquad \Phi = 0, \quad X > 1; \tag{2.26}$$

$$\Phi = 0, \quad \Phi_X = \Phi_{XXX} = \ldots = 0 \quad \text{for} \quad X = 0,\ Y \geqslant 0;$$

$$\Phi \to Q(X) = \int_0^X H\,\mathrm{d}X - \tfrac{1}{2}XH \qquad \text{exponentially as } Y \to \infty; \tag{2.27}$$

with $Q(1) = 0$, $H(1) = 0$, $G(1) = 0$, and $\Phi(1,0) = 0$. We also assume $Q(0) = 0$, which ensures that $\int_0^1 H\,\mathrm{d}X = 0$. The total mass of surfactant in the monolayer is $\mathscr{M} = \int_{-1}^1 G\,\mathrm{d}X$. The drop problem is, similarly,

$$\frac{1}{X}(\Phi_Y \Phi_{XY} - \Phi_X \Phi_{YY}) - \frac{\Phi_Y^2}{X^2} = \Phi_{YYY} + \tfrac{3}{8}X\Phi_{XY} + \tfrac{1}{2}Y\Phi_{YY} + \tfrac{1}{4}\Phi_Y, \tag{2.28}$$

$$\Phi = 0, \quad \Phi_Y = \tfrac{3}{8}X^2, \quad \Phi_{YY} = XG_X \quad \text{on } Y = 0, \quad 0 \leqslant X \leqslant 1; \quad \Phi = 0, \quad X > 1, \tag{2.29}$$

$$\Phi \to XQ(X) = \tfrac{5}{4}\int_0^X XH\,\mathrm{d}X - \tfrac{3}{8}X^2H \quad \text{exponentially as} \quad Y \to \infty. \tag{2.30}$$

The condition $Q(0) = 0$ ensures that $\int_0^1 XH\,\mathrm{d}X = 0$. The total mass of surfactant in the monolayer is $\mathscr{M} = 2\pi\int_0^1 XG\,\mathrm{d}X$.

3. A spreading monolayer strip or drop over deep fluid

The structure of the self-similar flow beneath a spreading monolayer is determined below by considering the neighbourhood of the origin, where there is an unsteady stretching flow (§3.1), and the leading edge, where there is a Blasius boundary layer (§3.2) and which is the most likely place for singular effects (e.g. surface diffusion, capillarity or surface contamination) to manifest themselves. The flow at the origin in the flat-surface formulation is considerably simpler than that in the front problem (Foda & Cox 1980; Dagan 1984). However, if free-surface deformation is permitted, the downward displacement of the interface is accomplished through the development of an inner layer, which shrinks relative to the monolayer, across which the similarity solution adjusts to symmetry boundary conditions (§3.1.1). Full numerical solutions of

the self-similar strip and drop problems, (2.25)–(2.27) and (2.28)–(2.30), are presented in §3.3.

3.1. *Structure at the origin: an unsteady stretching flow*

In the neighbourhood of the origin for the strip and drop problems, in their flat-surface formulations, the flow has a saddle-point structure, being driven by a horizontal surface velocity $u_s = ax/t$ for some constant a. It therefore falls into the class of boundary-layer flows on flat stretching surfaces, where the fluid is otherwise at rest. Although such flows have a fairly extensive literature (Stuart 1966; Bratukhin & Maurin 1967; Crane 1970; Wang 1971, 1984; Kuiken 1981; Banks 1983; Banks & Kuiken 1986; Surma Devi, Takhar & Nath 1986; Rajeswari, Kumari & Nath 1993; Smith 1994), to the author's knowledge the only directly relevant study is that due to Buckmaster (1973).

We may seek a series expansion of the flow in the neighbourhood of the origin. For the strip, symmetry conditions imply that U, G and H are even functions of X while Φ and Q are odd in X. We therefore pose expansions

$$\Phi = \tfrac{1}{2}g_0(Y)X + O(X^3), \quad Q(X) = \tfrac{1}{2}Q_0X + O(X^3),$$

$$H(X) = H_0 + O(X^2), \quad G(X) = G_0 + G_1X^2 + O(X^4).$$

On substituting these expansions into (2.25)–(2.27), we recover at leading order the problem

$$g_0'^2 - g_0g_0'' = 2g_0''' + 2g_0' + Yg_0'', \tag{3.1}$$

with boundary conditions

$$g_0(0) = 0, \qquad g_0'(0) = 1, \qquad g_0(Y) \to Q_0 \quad \text{exponentially as } Y \to \infty, \tag{3.2}$$

where $g_0''(0) = 4G_1$ and $Q_0 = H_0$. G_0 is undetermined at this stage, being related to the total mass of surfactant in the monolayer. This problem falls into the class of 'unsteady separated stagnation point (USSP) flows' (Ma & Hui 1990), and it can be considered a time-dependent generalization of the classical Hiemenz (1911) solution. The USSP flows can exhibit reversed flow and algebraic decay of the velocity field outside the boundary layer: g_0 is no exception, and can take the form

$$g_0 \sim Q_0 + C_0\left[\frac{1}{Y} - \frac{Q_0}{Y^2} + O\left(\frac{1}{Y^3}\right)\right] \qquad \text{as} \quad Y \to \infty$$

for some constant C_0. We must however impose exponential decay of the flow beneath the boundary layer (Goldstein 1965; Buckmaster 1973). The leading-order problem therefore has a unique solution, namely that for which $C_0 = 0$, which is the entirely forward flow for which there is the smallest total flow rate. This solution is shown with solid lines in figure 1; it is given by $G_1 \approx -0.05215$, so that $Q_0 = H_0 \approx 1.3422$. As Buckmaster (1973) found, a series of problems can be formulated at higher orders in X, but each contains an undetermined constant. It is not possible to construct a solution by advancing in the positive X-direction, a consequence of the parabolic nature of the governing equations.

A similar argument may be followed for the drop case. Setting $\Phi \sim \frac{3}{8}g_0(Y)X^2$, $Q \sim \frac{3}{8}Q_0X$ at leading order in X, with H and G as above, yields

$$\tfrac{3}{8}\left(g_0'^2 - 2g_0g_0''\right) = g_0''' + g_0' + \tfrac{1}{2}Yg_0'',$$

with the same boundary conditions as the strip case but with $g_0''(0) = \frac{16}{3}G_1$. The unique

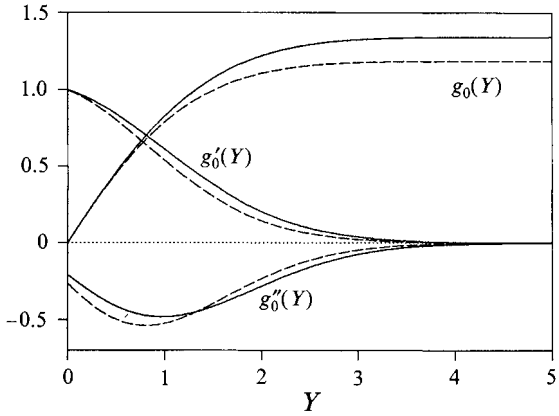

FIGURE 1. The flow at the origin, showing the function $g_0(Y)$ and its derivatives for a strip (——) and a drop (— —); $g_0'(Y)$ shows the profile of the horizontal component of velocity.

solution exhibiting exponential decay is given by $Q_0 = \frac{2}{3}H_0 \approx 1.1842$, $G_1 \approx -0.04984$, and is shown by dashed lines in figure 1.

3.1.1. *Unsteady inner layer at the origin*

Having determined the nature of the flat-surface problem near the origin, we can consider how it transforms to the deforming-surface problem. The full solution giving $Q(X)$ will be determined in §3.3 below. From this, we can determine the corresponding T-independent free-surface shape $H(X)$, which comes from integrating the steady version of the kinematic condition (2.13),

$$H(X) = \frac{2(n+2)}{3} X^{(n+2)/3} \int_X^1 X^{-(n+5)/3} \partial_X Q \, \mathrm{d}X.$$

The contribution to H from the upper limit of integration at $X = 1$ is of the form $H = A_0 X^{(n+2)/3}$, for some constant $A_0 \neq 0$, so that after solving the complete problem we have $H = H_0 + A_0 X^{(n+2)/3} + O(X^2)$ near the origin. Because $H_0 > 0$, the free surface will be displaced downwards at the origin. However, this solution fails to satisfy the symmetry condition $H_X(0) = 0$ that applies for the strip and drop configurations; it is of course to be expected that a similarity solution might fail at one end of its domain. Exactly this behaviour was observed by JG for similarity solutions of the analogous thin-film problems. In that case, numerical solutions of the full, unsteady equations exhibited an unsteady inner layer at the origin, across which solutions adjust to the symmetry boundary conditions; the observed scaling of this inner layer was supported by theoretical arguments. We hypothesize that in the present case an unsteady inner layer exists also, and use similar reasoning to establish its magnitude.

We therefore return to the time-dependent kinematic condition, $h_t = \partial_x q$, which in transformed variables is given by (2.13),

$$\partial_X Q = T H_T + \tfrac{1}{2}\left(H - \frac{3}{n+2} X H_X\right).$$

Integrating this equation to find $H(X, T)$ for a given $Q(X)$, again imposing the

boundary conditions $H(1,T)=0$, $Q(1)=0$, we have now an additional contribution to H,

$$H(X,T)=\frac{2(n+2)}{3}X^{(n+2)/3}\int_X^1 X^{-(n+5)/3}\partial_X Q\,\mathrm{d}X+T^{-1/2}\tilde{h}\left(XT^{3/[2(n+2)]}\right). \tag{3.3}$$

Transforming back to the original variables, the complementary function $\tilde{h}$ is a function of x alone, i.e. it represents a steady film shape, as would be expected from integrating $h_t=\partial_x q$. The symmetry condition for a strip (with $n=1$) can now be satisfied provided $\tilde{h}$ satisfies

$$\tilde{h}'(0)=-A_0(<0),\quad \tilde{h}(\infty)\to 0,\quad \tilde{h}(0)<0\quad\text{and}\quad\int_0^\infty \tilde{h}\,\mathrm{d}x=0.$$

Likewise, for a drop we require $\tilde{h}'\sim-\frac{4}{3}A_0x$ as $x\to 0$, $\tilde{h}(x)\to 0$ as $x\to\infty$, $\tilde{h}(0)<0$, and $\int_0^\infty x\tilde{h}\,\mathrm{d}x=0$. Thus in the frame of the monolayer, an unsteady boundary layer exists at the origin, which (according to (3.3)) shrinks in magnitude like $T^{-1/2}$ for a strip, and $T^{-3/8}$ for a drop. The form of $\tilde{h}$ cannot be determined directly, but must be deduced from a solution of the full time-dependent initial-value problem.

3.2. *Structure at the leading edge*

It is straightforward to follow Buckmaster (1973) or Foda & Cox (1980) to establish the Blasius boundary-layer structure at the monolayer's leading edge. Here, we extend this analysis briefly to consider additional singular effects such as diffusion, gravity, capillarity and surface contamination.

We make the following expansion about the leading edge at $X=1$. Suppose that $\hat{\epsilon}\ll 1$, and rescale as follows: $X=1+\hat{\epsilon}\hat{X}$, $Y=\hat{\epsilon}^{1/2}\hat{Y}$, $\Phi=\hat{\epsilon}^{1/2}\hat{\phi}$, $G=\hat{\epsilon}^{1/2}\hat{G}$, $H=\hat{\epsilon}^{1/2}\hat{H}$ and $Q=\hat{\epsilon}^{1/2}\hat{Q}$. This choice of scaling ensures an appropriate leading-order balance of viscous and Marangoni forces; the lengthscale $\hat{\epsilon}$ must be chosen to include singular effects at this order. To leading order (2.25) and (2.28) become

$$\hat{\phi}_{\hat{Y}}\hat{\phi}_{\hat{X}\hat{Y}}-\hat{\phi}_{\hat{X}}\hat{\phi}_{\hat{Y}\hat{Y}}=\hat{\phi}_{\hat{Y}\hat{Y}\hat{Y}}+\frac{3}{2(n+2)}\hat{\phi}_{\hat{X}\hat{Y}}, \tag{3.4}$$

subject to

$$\left.\begin{aligned}\hat{\phi}&=0\\ \left[\left(\hat{\phi}_{\hat{Y}}-\frac{3}{2(n+2)}\right)\hat{G}\right]_{\hat{X}}&=(\hat{\mathscr{D}}/\hat{\epsilon})\partial_{\hat{X}}\hat{G}_{\hat{X}}\\ \hat{\phi}_{\hat{Y}\hat{Y}}&=\hat{G}_{\hat{X}}\end{aligned}\right\}\qquad\text{on }\hat{Y}=0,$$

$$\hat{\phi}\to\hat{Q}=-\frac{3}{2(n+2)}\hat{H}(\hat{X})\qquad\text{as }\hat{Y}\to\infty,$$

where surface diffusion $\hat{\mathscr{D}}$ (see (2.14)) has been re-inserted into the surfactant transport equation. If it is assumed that $\hat{H}\to 0$, $\hat{G}\to\hat{G}_\infty$ and $\hat{Q}\to 0$ as $\hat{X}\to\infty$, then we can integrate the boundary-layer equation with respect to $\hat{Y}$ and $\hat{X}$ to derive the momentum integral equation

$$\int_0^\infty\hat{\phi}_{\hat{Y}}^2\,\mathrm{d}\hat{Y}+(\hat{G}-\hat{G}_\infty)=\frac{3}{2(n+2)}\hat{Q}.$$

Since $\hat{G} \geqslant \hat{G}_\infty$, $\hat{Q} \geqslant 0$ so that $\hat{H} \leqslant 0$, i.e. the free surface is elevated over this region.

We consider first the limit in which $\hat{\mathscr{D}} = 0$ and $\hat{G}_\infty = 0$. Then the surfactant transport equation has the following solution: $\hat{G} = 0$ for $\hat{X} > 0$ and $\hat{\phi}_{\hat{Y}} = 3/[2(n+2)]$ for $\hat{X} < 0$. For $\hat{X} > 0$, the fluid is undisturbed, while for $\hat{X} < 0$, we recover the Blasius boundary-layer solution. Defining $y = \hat{Y}/(-\hat{X})^{1/2}$, and letting $\hat{G} = \hat{G}_0(-\hat{X})^{1/2}$, $\hat{Q} = \hat{Q}_0(-\hat{X})^{1/2}$, $\hat{H} = \hat{H}_0(-\hat{X})^{1/2}$, $\hat{\phi} = (-\hat{X})^{1/2}\hat{\phi}_0(y)$, we obtain for $\hat{X} < 0$

$$\hat{\phi}_0\hat{\phi}_{0yy} = 2\hat{\phi}_{0yyy} + \frac{3}{2(n+2)}y\hat{\phi}_{0yy}, \tag{3.5}$$

while the boundary conditions become $\hat{\phi}_0 = 0$, $\hat{\phi}_{0y} = 3/[2(n+2)]$ and $\hat{\phi}_{0yy} = -\frac{1}{2}\hat{G}_0$ on $y = 0$, with $\hat{\phi}_0 \to \hat{Q}_0 = -3\hat{H}_0/[2(n+2)]$ as $y \to \infty$. Putting $\phi_0 = \tilde{\phi} + (3y/[2(n+2)])$ yields the Blasius problem for $\tilde{\phi}$, i.e. $\tilde{\phi}_{yyy} = \frac{1}{2}\tilde{\phi}\tilde{\phi}_{yy}$, with $\tilde{\phi} \sim o(y)$ as $y \to 0$ and $\tilde{\phi} + (3y/[2(n+2)]) \to \hat{Q}_0$ as $y \to \infty$. Thus $\hat{H}_0 = -2\left[(n+2)/3\right]^{1/2}\beta_1$ where $\beta_1 \approx 1.21678$ (Van Dyke 1975). Thus the free surface is displaced upwards, and has infinite gradient at $X = 1$. The corresponding value of $\hat{G}_0$ is $\frac{1}{2}\left[3/(n+2)\right]^{3/2}\alpha_1$ where $\alpha_1 \approx 0.46960$. There is a singularity in the shear stress at the leading edge of the monolayer, and correspondingly an infinite vertical velocity. The film deformation at the leading edge is slightly more severe for the drop, although the shear stress is weaker; the velocity field decays exponentially as $y \to \infty$, as required.

3.2.1. *Inner layers at the leading edge*

If we re-introduce the pressure gradient in the momentum equation (see §2.2), (3.4) becomes

$$\hat{\phi}_{\hat{Y}}\hat{\phi}_{\hat{X}\hat{Y}} - \hat{\phi}_{\hat{X}}\hat{\phi}_{\hat{Y}\hat{Y}} = \hat{\phi}_{\hat{Y}\hat{Y}\hat{Y}} + \frac{3}{2(n+2)}\hat{\phi}_{\hat{X}\hat{Y}} + \hat{\epsilon}^{1/2}\hat{\mathscr{G}}\hat{H}_{\hat{X}} - \hat{\epsilon}^{-3/2}\hat{\mathscr{S}}\hat{H}_{\hat{X}\hat{X}\hat{X}}.$$

We can now identify the lengthscales over which weak, singular effects operate by choosing values of $\hat{\epsilon}$ making the appropriate terms in the governing equations $O(1)$. Evidently, the diffusive, gravitational and capillary lengthscales ($\hat{\epsilon} = X_{\mathscr{D}}$, $X_{\mathscr{G}}$ and $X_{\mathscr{S}}$ respectively) are given by

$$X_{\mathscr{D}} = \hat{\mathscr{D}}, \quad X_{\mathscr{G}} = \hat{\mathscr{G}}^{-2}, \quad X_{\mathscr{S}} = \hat{\mathscr{S}}^{2/3}.$$

Provided $\hat{\mathscr{D}} \ll 1$, diffusive effects are confined to a thin inner layer which grows at the same rate as the monolayer for a strip, while it shrinks for a front and grows for a drop. For $\hat{\mathscr{S}} \ll 1$, capillary forces also operate over a thin region, which shrinks relative to the monolayer for a front but grows for a strip or drop. $X_{\mathscr{G}}$ is not small, however, even for $\hat{\mathscr{G}} \ll 1$, indicating that gravitational effects are not confined to the leading edge, but act as an unsteady regular perturbation over a substantial proportion (if not all) of the monolayer. These findings are all consistent with the observation (in §2.2) that a front can be dominated in finite time by gravity, a strip by gravity or capillarity and a drop by all three effects. The capillary boundary layer at the leading edge will behave in a quasi-steady manner, via a viscous–inviscid interaction: the curvature of the free surface generates a pressure gradient, which is transmitted through the boundary layer and drives an irrotational flow at depth, which in turn is coupled to the boundary-layer flow. It is likely that a weak wavetrain will be generated in the free surface in $\hat{X} > 0$, in a manner similar to that identified in JG for monolayers on thin films.

A further potentially significant mechanism by which the singularity at the leading edge could be smoothed is through surface contamination of the undisturbed

interface. Suppose, ahead of the advancing monolayer, there is a uniform monolayer of some low, dimensional, concentration Γ_∞. The corresponding, nondimensional, scaled concentration is (from §2.1) $G_\infty = \left(t^{3n}/\mathscr{M}^4\mathscr{R}^n\right)^{1/[2(n+2)]}(\Gamma_\infty/\Gamma_0)$. Imposing the condition that $\hat{G} \to \hat{G}_\infty = 1$ as $\hat{X} \to \infty$, we require that $\hat{\epsilon} = G_\infty^2$, so that the lengthscale over which the contaminant operates is

$$X_\infty = \left(\frac{t^{3n}}{\mathscr{M}^4\mathscr{R}^n}\right)^{1/(n+2)}\left(\frac{\Gamma_\infty}{\Gamma_0}\right)^2. \tag{3.6}$$

Thus for a strip or a drop, this sublayer grows with respect to time, and the effects of the contaminant may dominate the complete flow at sufficiently large times (see §4 below). While the inner layer remains small relative to the length of the monolayer, it behaves quasi-steadily (see JG, who found its thin-layer analogue). Its structure in the deep-layer case is essentially that determined by Harper & Dixon (1974), who computed the flow for a monolayer advancing against a steady stream (corresponding to the case $n = -\frac{1}{2}$) using a momentum-integral approximation. The same method can readily be extended to unsteady monolayer spreading (i.e. other values of n), and it can be used to determine the structure of the diffusive sublayer also.

3.3. *Full numerical solution*

To obtain a numerical solution of the strip and drop problems, the governing equations (2.25)–(2.27) and (2.28)–(2.30) were recast in rescaled coordinates before being solved by a finite-difference method, marching from the leading edge towards the origin. For details, see Appendix A.

The solution of the strip problem is shown in figures 2(*a*) and 3. Figure 2(*a*) shows that the surfactant distribution $G(X)$ diminishes monotonically across the monolayer, such that the shear stress at the free surface $-G_X$ increases from zero at the origin to a singularity at the leading edge. The instantaneous flow rate $Q(X)$ increases roughly linearly across the upstream 75% of the monolayer, and also has the anticipated singular form at $X = 1$. The displacement thickness $\delta(X) = Q/U_s$ where $U_s = \frac{1}{2}X$, a measure of the depth to which vorticity penetrates downwards into the fluid, is roughly uniform over the upstream half of the monolayer, decreasing rapidly near the leading edge. This is evident also from the stream-function distribution in figure 3(*a*), which shows the flow in its flat-surface formulation. There is a concentrated downward flow near the leading edge at $X = 1$, and an upward flow generated by the stretching free surface over the upstream 75% of the monolayer. When reformulated to allow displacement of the free surface, (figure 3*b*), we see that the free surface is displaced downwards over $0 < X < 0.427$, and upwards further downstream. Note that $H(X)$ is linear as $X \to 0$, requiring an unsteady boundary layer to match to the symmetry boundary conditions (§3.1.1). The spreading monolayer drop has a very similar distribution (figure 2*b*). Again, the displacement thickness δ is almost uniform over the upstream half of the monolayer. The free-surface displacement is now more nonlinear, with a greater depression at the origin and a weaker elevation towards the leading edge. The value of $\mathscr{M}$ corresponding to each flow is as follows: for the strip $\mathscr{M} \approx 0.215$, with $G(0) \approx 0.1306$; for the drop, $\mathscr{M} \approx 0.198$, with $G(0) \approx 0.0921$.

The stream-function distributions in figure 3 help demonstrate the importance of free-surface displacement: in the absence of any pressure gradients, both flows are solutions of the governing equations, and yet only one is likely to be realized. To determine which, suppose that a monolayer is advancing over fluid of finite depth

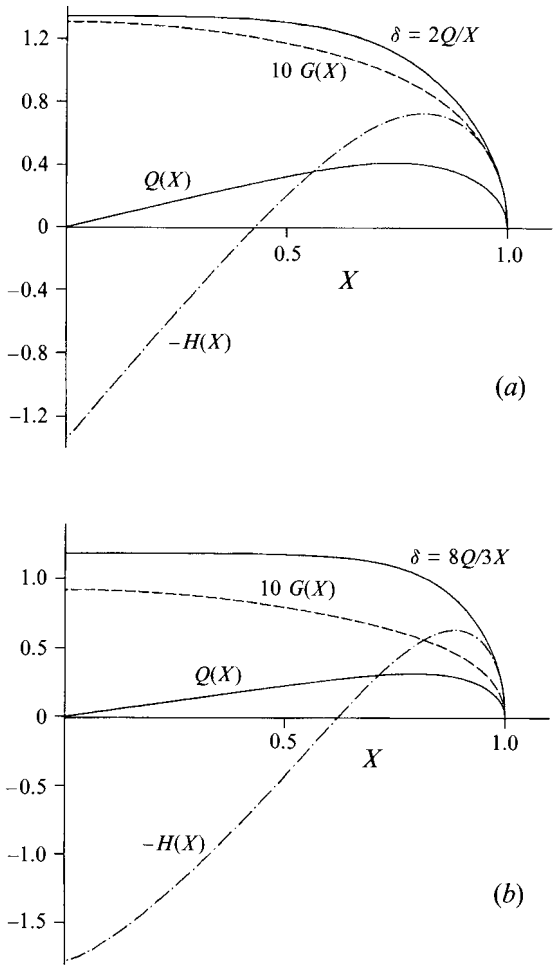

FIGURE 2. The surfactant distribution $G(X)$, instantaneous flow rate $Q(X)$, displacement thickness $\delta(X)$ and free-surface displacement $H(X)$ for (*a*) a strip and (*b*) a drop.

H_0, where the lower boundary of the fluid layer is well beneath the rotational region of the flow. If the free surface deforms freely (figure 3*b*), the lower boundary has no effect on the flow, since all motion decays exponentially in the downward direction. If the free surface is horizontal, however (figure 3*a*), then the irrotational flow that develops outside the boundary layer will drive a second unsteady boundary-layer flow just above the solid boundary. This in turn may influence the flow at the free surface; it is certainly the case that the net dissipation in the flat-surface case will be substantially greater than in the deforming-surface case. Gravity or capillarity are the forces that must provide the additional energy necessary to drive this second boundary layer.

The influence of finite depth effects are examined in more detail in §5 below. Before this, however, the potentially significant large-time influence of surface contamination is considered.

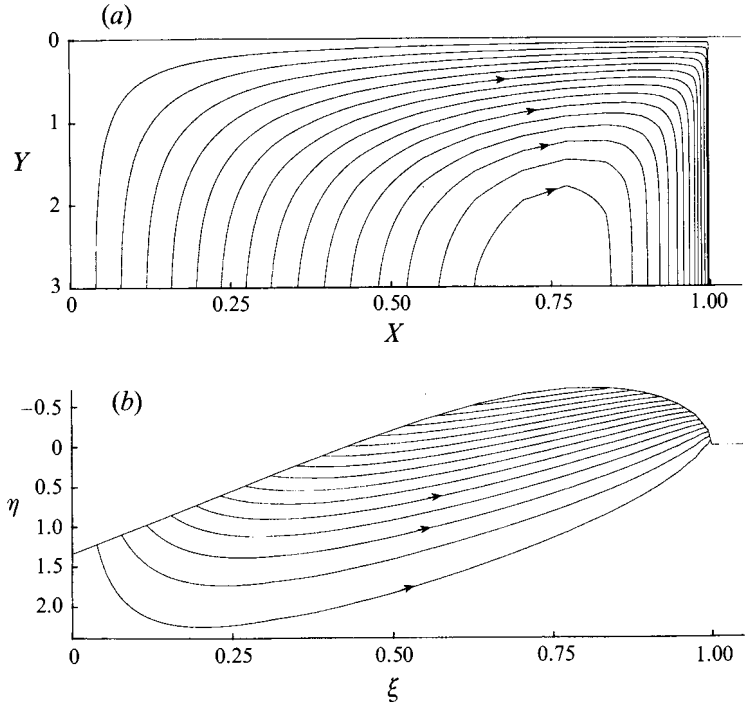

FIGURE 3. The stream functions for a spreading monolayer strip: (*a*) the similarity solution $\Phi(X, Y)$, for the flat free-surface problem; (*b*) its analogue $\psi(\xi, \eta)$, for the freely deforming free-surface case. Arrows indicate the direction of the flow.

4. Spreading over a contaminated interface

Consider now the case in which a monolayer strip or drop spreads over an interface that is already contaminated with a uniform distribution of surfactant of constant dimensional concentration Γ_∞. (This concentration can be taken as the reference scale Γ_0 in deriving (2.1), (2.8) and (2.4) (see §2.1); it is assumed the parameter $\mathscr{M}$ retains its scaling on some source strength $\Gamma_0 > \Gamma_\infty$ in (2.6), however.) The key aspects of the dynamics have already been explored in thin-layer studies (JG; Espinosa *et al.* 1993; Grotberg *et al.* 1995). Initially, the effect of contaminant is confined to a growing sublayer at the deposited monolayer's leading edge (§3.2). Once this layer has grown to a magnitude comparable with the length of the monolayer, i.e. once $X_\infty = O(1)$ (see (3.6)), the time-dependence of the entire flow is altered. Below, it is shown for deep layers that the Eulerian velocity field is self-similar at large times, with disturbances spreading like (1.2), dependent not on the source strength $\mathscr{M}$ but on the level of contamination Γ_∞. Paradoxically, this suggests that a deposited surfactant monolayer might spread rapidly even for $\mathscr{M} \ll 1$, a limit in which the energy available to drive the spreading is vanishingly small. Grotberg *et al.* (1995) have shown, however, that the Lagrangian path of a surface fluid particle, representing the distance travelled by the deposited monolayer (in the absence of surface diffusion), *is* dependent on $\mathscr{M}$, so that there is no transport of deposited material in the limit $\mathscr{M} \to 0$.

At the late stages of spreading of a strip or a drop, or for the spreading of a front from a relatively weak source, the surfactant concentration will everywhere be only slightly in excess of its nondimensional value at infinity $\Gamma = 1$. We therefore pose an

expansion

$$\Gamma(x,t) = 1 + \delta\hat{\Gamma} + O(\delta^2), \quad u(x,y,t) = \delta\hat{u} + O(\delta^2), \quad w(x,y,t) = \delta\hat{w} + O(\delta^2), \quad (4.1)$$

where $\delta \ll 1$. In such an expansion any free surface displacement must be $O(\delta)$, but since we are concerned with large-time behaviour, and have shown that displacements may grow like $t^{1/2}$, it is necessary to restrict attention to the case in which restoring forces keep the free surface horizontal. Substituting (4.1) into (2.1), (2.4) (with $\mathscr{D} = 0$) and (2.8) yields at $O(\delta)$ an unsteady problem that is linear in $\hat{u}(x,z,t)$ and $\hat{\Gamma}(x,t)$,

$$\hat{u}_t = \mathscr{R}^{-1}\hat{u}_{zz} \quad \text{in } z \geqslant 0, \quad (4.2)$$

$$\hat{\Gamma}_t + \partial_x\hat{u} = 0, \quad \hat{u}_z = \hat{\Gamma}_x \quad \text{on} \quad z = 0, \qquad \hat{u} \to 0 \quad \text{as} \quad z \to \infty. \quad (4.3)$$

The vertical velocity field need not be considered at leading order. A scaling analysis reveals the following relationships:

$$x \sim \left(t^3/\mathscr{R}\right)^{1/4}, \qquad z \sim (t/\mathscr{R})^{1/2}, \qquad \hat{u} \sim \hat{\Gamma}/(\mathscr{R}t)^{1/4}.$$

For consistency, we require that $x \gg z$, i.e. $t \gg 1/\mathscr{R}$, which is readily satisfied at large times. The x-scaling in dimensional terms is equivalent to (1.2). Thus, irrespective of the geometry or strength of the monolayer distribution, spreading proceeds like $t^{3/4}$.

New variables may be defined to take account of this self-similar structure. Since $\hat{\Gamma} \sim \mathscr{M}x^{-n}$, we have $\hat{\Gamma} \sim t^{-3n/4}$, for $n = 0$, 1 or 2 respectively. Writing

$$x = \left(t^3/\mathscr{R}\right)^{1/4} X, \qquad z = (t/\mathscr{R})^{1/2} Z, \qquad t = T,$$

$$\hat{\Gamma}(x,t) = \mathscr{M}\left(\mathscr{R}/t^3\right)^{n/4} G(X,T), \qquad \hat{u}(x,z,t) = \left(\mathscr{M}\mathscr{R}^{(n-1)/4}/t^{(1+3n)/4}\right) U(X,Z,T),$$

(4.2) and (4.3) in these rescaled, nondimensional variables becomes

$$U_{ZZ} + \tfrac{1}{4}(1+3n)U + \tfrac{3}{4}XU_X + \tfrac{1}{2}ZU_Z = TU_T \quad \text{in } Z \geqslant 0, \quad (4.4)$$

$$TG_T + \partial_X U = \tfrac{3}{4}(nG + XG_X), \quad U_Z = G_X \quad \text{on } Z = 0, \quad (4.5)$$

$$U \to 0 \quad \text{as } Z \to \infty. \quad (4.6)$$

The integral form of the momentum equation is obtained by integrating (4.4) with respect to Z,

$$-4TQ_T + (3n-1)Q + 3XQ_X = 4G_X \quad \text{where} \quad Q(X,T) = \int_0^\infty U \, \mathrm{d}Z. \quad (4.7)$$

Integrating with respect to X and imposing the condition that $Q \to 0$ as $X \to \infty$ gives

$$Q(X,T) = \frac{4}{3X^{n-(1/3)}} \int_\infty^X X^{n-(4/3)} G_X \, \mathrm{d}X + T^{(1-3n)/4}\hat{q}(XT^{3/4}),$$

so that Q is determined up to some arbitrary quantity $\hat{q}$, which represents a steady flow in the laboratory frame. This complementary function is presumably determined by the initial conditions and the boundary conditions at $X = 0$. The contribution to Q represented by the limit of integration at $X \to \infty$ introduces a singularity $Q \sim AX^{(1/3)-n}$ as $X \to 0$, so we anticipate that once again the similarity solution will fail to satisfy realistic boundary conditions at $X = 0$. If $A = O(1)$, this singularity can be accommodated by the unsteady component $\hat{q}$, provided $\hat{q}(\xi) \sim \xi^{n-(1/3)}$ as

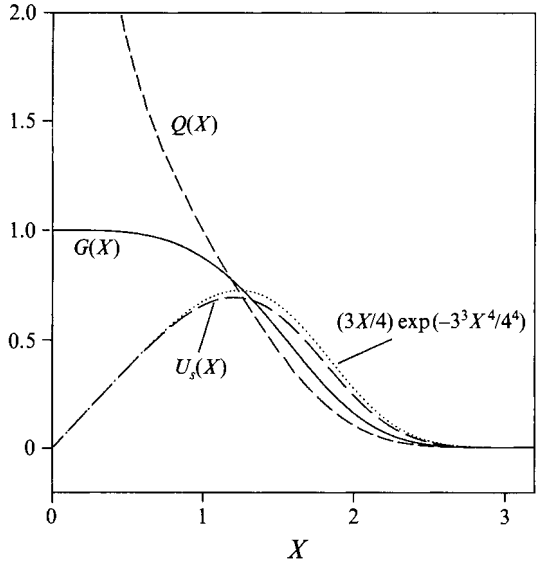

FIGURE 4. A spreading strip on a contaminated interface.

$\xi \to \infty$, so that there will be a boundary layer at the origin, which (as in §3.1.1) is unsteady with respect to the monolayer but is steady in the original coordinate system.

Similarity solutions of (4.2) and (4.3), i.e. T-independent solutions of (4.4)–(4.6) for the strip and drop flows, have been computed using an integral approximation, the details of which are described in Appendix B. The strip solution is shown in figure 4; the drop solution, not shown, is very similar. As anticipated, the flow rate $Q(X)$ (and hence the flow's displacement thickness) are singular at the origin. The perturbation surfactant distribution $G(X)$ and the surface velocity $U_s(X) = \frac{3}{4}XG$ are well-behaved there, however. The surfactant distribution no longer has a singularity at its leading edge (as in figure 2), but instead diminishes smoothly to a uniform value as $X \to \infty$, while $U_s(X)$ (which is well-approximated by a simple exponential function, see figure 4) rises almost linearly to a maximum near $X = 1.3$, before falling rapidly to zero by $X \approx 3$. Whereas the clean-surface flows (figures 2 and 3) are characterized by stretching of the monolayer along its entire length (i.e. $U_{sX} > 0$ for $0 < X < 1$), the effect of contamination is to introduce a significant region of free-surface compression (where $U_{sX} < 0$). Much of the flow is therefore driven by a mechanism unlike that in the clean-surface case, namely through the generation of surface tension gradients arising through compression of the contaminant material. For a more detailed discussion of such behaviour see Grotberg *et al.* (1995).

5. Finite-depth effects

It is now evident that a localized monolayer, spreading over fluid of finite depth, spreads initially like $t^{3/2(n+2)}$ (see (1.1)), generating a high-Reynolds number boundary-layer flow (figure 3*b*), until the effect of the lower boundary is first felt. Spreading then enters a more complex intermediate phase which persists until the monolayer length greatly exceeds the depth of the fluid layer. Thereafter, a lubrication-theory approximation is appropriate, and spreading proceeds like $t^{1/(n+2)}$ (JG), with a predominantly

viscous flow. Below, a simplified one-dimensional model of spreading is presented which characterizes the dominant features of the dynamics of this intermediate stage, without necessitating a full numerical solution of an unsteady two-dimensional free-boundary problem.

5.1. *The one-dimensional model*

The essence of the long-wavelength monolayer-spreading problem is contained in the two (dimensional) free-surface boundary conditions

$$\Gamma_t + \nabla_s \cdot (\boldsymbol{u}_s \Gamma) = 0, \qquad \mu(\boldsymbol{n} \cdot \nabla)\boldsymbol{u}|_s = -\left|\frac{\mathrm{d}\sigma}{\mathrm{d}\Gamma}\right| \nabla_s \Gamma. \tag{5.1}$$

The similarity solutions given in §3 and JG provide accurate spatial distributions of Γ and $\boldsymbol{u}$ in suitable asymptotic regimes, but rely on the assumption that these variables have a specific time-dependence. An alternative approach, which captures fully unsteady behaviour at the expense of some spatial structure, is to write

$$(\boldsymbol{n} \cdot \nabla)\boldsymbol{u}|_s \approx \frac{\boldsymbol{u}_s}{\mathscr{Z}}, \tag{5.2}$$

decoupling the flow problem from the surfactant transport problem. The quantity $\mathscr{Z}(x,t)$ is the penetration depth of vorticity created at the free surface, which can be chosen to suit the situation. We concentrate primarily on ensuring that $\mathscr{Z}$ is of the correct order of magnitude. The shape and magnitude of film deformations will weakly influence $\mathscr{Z}$, but such effects are neglected at this stage.

The reduced model may be nondimensionalized just as in §2, with x scaled on L_0, $\mathscr{Z}$ on ϵL_0, for some $\epsilon \ll 1$, etc. This leaves two nondimensional parameters, Re and $\mathscr{M}$; for spreading over a clean interface, the parameter $\mathscr{M}$ in (2.6) can be set to unity by rescaling $x \to x/\mathscr{M}^{1/(n+2)}$, $\Gamma \to \Gamma/\mathscr{M}^{2/(n+2)}$. Equations (5.1) and (5.2) then reduce to a nonlinear diffusion equation

$$\Gamma_t = \partial_x(\mathscr{Z}\Gamma\Gamma_x). \tag{5.3}$$

To determine the accuracy of this simplified model, we first compare predictions for thin-film and deep-layer flows with existing results.

For flow over a thin film of mean depth H_0, we set $\epsilon = H_0/L_0$ and $\mathscr{Z} = 1$. Then (5.3) yields similarity solutions of the form $\Gamma(x,t) = G(x/L)/L^n$, describing localized monolayers on uncontaminated interfaces, with $L(t) \propto t^{1/(n+2)}$ as required. The corresponding Γ-distribution for a strip, say, with $\int_0^1 G\,\mathrm{d}x = 1$,

$$\Gamma(x,t) = \tfrac{1}{2}L\dot{L}\left(1 - \frac{x^2}{L^2}\right), \quad u_s = \frac{x}{3t} \quad \text{for} \quad 0 \leqslant x \leqslant L(t) = (9t)^{1/3}, \tag{5.4}$$

which has a shape almost indistinguishable from the curve labelled $L = 8$ in figure 5, compares reasonably well with the exact self-similar solution derived using lubrication theory by JG, given by $\Gamma(x,t) = \frac{1}{2}L\dot{L}[1-(x/L)]$ with the leading edge at $L = (12t)^{1/3}$.

For deep-layer flow, vorticity penetrates a dimensional depth of order $(\nu t)^{1/2}$ (see §1), so we choose $\epsilon = Re^{-1/2}$. Setting $\mathscr{Z} = t^{1/2}$ is sufficient to obtain similarity solutions with the appropriate time-dependence (i.e. $L(t) \propto t^{3/2(n+2)}$). However, these solutions fail to capture the important Blasius boundary-layer structure at the monolayer's leading edge, shown clearly in the curves for $G(X)$ in figure 2, warranting a refinement of $\mathscr{Z}$, as follows. The monolayer lies in $0 < x < L(t)$, where L remains to be determined. Near the leading edge, which moves with speed $\dot{L}$, the penetration depth

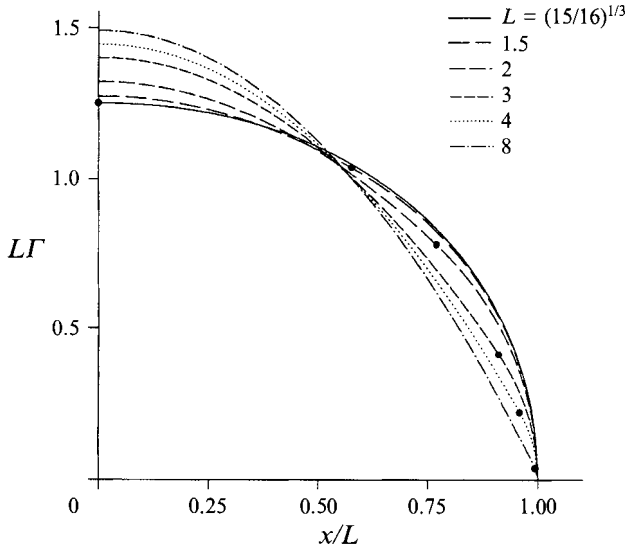

FIGURE 5. Surfactant distributions predicted by the simplified model (5.3) and (5.7) for a spreading monolayer strip over fluid of finite depth; bullets show the boundary between the viscous and inertial regions at $x = X(t)$. Plots are given at $t = \frac{1}{2}$, 0.652, 1.42, 4.44, 10.9 and 133 for $L = (15/16)^{1/3}$, 1.5, 2, 3, 4 and 8 respectively.

of vorticity $\delta(X)$ (figure 2) has a typical parabolic shape. This can be represented by

$$\mathscr{Z} = c\left(\frac{(L-x)}{\dot{L}}\right)^{1/2} \tag{5.5}$$

for some constant c, which for simplicity is set to unity. Substituting (5.5) into (5.3), along with a self-similar surfactant distribution $\Gamma(x,t) = G(x/L)/L^n$, we find that solutions exist provided $\dot{L}^3 L^{2n+1} =$ constant, i.e. $L \propto t^{3/[2(n+2)]}$ as required. The similarity solution for a strip with $\int_0^1 G\,\mathrm{d}x = 1$ is

$$\Gamma = \frac{4\dot{L}^{3/2}}{3L}(L-x)^{1/2}(L+\tfrac{1}{2}x), \quad u_s = \frac{x}{2t} \quad \text{for} \quad 0 \leqslant x \leqslant L = \left(\tfrac{15}{16}\right)^{1/3}(2t)^{1/2}. \tag{5.6}$$

This distribution is shown by the solid curve in figure 5: it is clearly in good qualitative agreement with the exact solution (see $G(X)$ in figure 2*a*).

5.2. *Modelling finite-depth spreading*

Having established that the one-dimensional model captures the time-dependence of the thin-layer and deep-layer flows exactly, and their spatial structures approximately, we turn now to the intermediate finite-depth case. Consider a localized monolayer spreading on a uniform fluid layer of depth H_0 where, at least initially, $L_0 \ll H_0$. We again nondimensionalize using $\epsilon = H_0/L_0$, and set $\mathscr{R} = \epsilon^2 Re$. The parameter ϵ is no longer regarded as small: the applicability of the long-wavelength assumption will be reconsidered below.

As the monolayer begins to spread, vorticity diffuses downward, so that after a (dimensional) time of $O(H_0^2/\nu)$ the presence of the wall becomes important. Thereafter, the spreading monolayer can be split into two distinct parts: region I ($0 < x < X(t)$), in which vorticity has diffused to the lower boundary, so $\mathscr{Z} = 1$; and region II ($X(t) < x < L(t)$), in which vorticity created at the free surface is diffusing down

into the fluid, uninfluenced by the solid boundary, so that (5.5) (suitably scaled) may be used, i.e. $\mathscr{Z} = [(L-x)/\mathscr{R}\dot{L}]^{1/2}$. Imposing continuity of $\mathscr{Z}$ at $x = X$ implies that $X(t) = L - \mathscr{R}\dot{L}$. The two parameters $\mathscr{M}$ and $\mathscr{R}$ can then be eliminated through a rescaling:

$$x = (\mathscr{M}\mathscr{R})^{1/(n+2)}\tilde{x}, \quad t = \mathscr{R}\tilde{t}, \quad \Gamma = (\mathscr{M}^2/\mathscr{R}^n)^{1/(n+2)}\tilde{\Gamma}.$$

The time $\tilde{t}$ is based on the natural viscous timescale $T_v = H_0^2/\nu$, so that vorticity reaches the boundary for $\tilde{t} = O(1)$. The timescale of the deep-layer flow is $O((L_0/H_0)^2 T_v)$ (with $L_0 \ll H_0$, see §2), corresponding to $\tilde{t} \ll 1$. The thin-layer flow evolves over a timescale $O(T_v/\mathscr{R})$ where $\mathscr{R} \ll 1$ (JG), corresponding to $\tilde{t} \gg 1$. Thus, dropping the tildes, finite-depth effects are represented by (5.3) with

$$\mathscr{Z} = \begin{cases} 1, & 0 < x < X(t), \\ [(L-x)/\dot{L}]^{1/2}, & X(t) < x < L(t), \end{cases} \qquad \text{where} \qquad X(t) = L - \dot{L} \tag{5.7}$$

provided, of course, that $X(t) \geqslant 0$. Surfactant mass is distributed between regions I and II such that, for a strip, say, $M_I + M_{II} = 1$ where $M_I = \int_0^{X(t)} \Gamma \, dx$, $M_{II} = \int_{X(t)}^{L(t)} \Gamma \, dx$, with the mass flux J from region II into region I at $x = X(t)$ given by

$$J = (\dot{X} + \mathscr{Z}\Gamma_x)\Gamma\Big|_{x=X(t)},$$

so that $M_{It} = J$, $M_{IIt} = -J$. Because $\mathscr{Z}$ is continuous at $x = X$, Γ_x must be continuous there too. The long-wavelength approximation, which applies within regions I and II, should also be satisfied at their boundary because Γ is sufficiently smooth there.

5.3. *Self-similar solution*

Both the thin-layer and deep-layer spreading regimes for a strip, say (5.4), (5.6), are characterized by a surface velocity of the form $u_s = \lambda x/t$, for some constant λ. To determine the evolution of the monolayer in the intermediate regime, we therefore assume that $u_s = \dot{L}x/L$ for some $L(t)$. It may readily be shown from the transport equation $\Gamma_t + \partial_x(u_s\Gamma) = 0$ (by the method of characteristics) that this assumption is equivalent to assuming a self-similar distribution $\Gamma(x,t) = G(x/L)/L^n$, $(n = 1, 2)$, for some function G. The Γ-distribution is readily calculated using $\Gamma_x = -u_s/\mathscr{Z}$.

The strip solution is determined as follows. Starting in region II, imposing $\Gamma(L,t) = 0$, we recover the Γ-distribution in (5.6) for $X \leqslant x \leqslant L$, so that

$$M_{II} = \frac{4}{15}\frac{\dot{L}^{3/2}}{L}(4L + X)(L - X)^{3/2}.$$

Initially, before vorticity has diffused down to the boundary, $X = 0$ and $M_{II} = 1$, and hence we recover (5.6), valid for $0 < t \leqslant \frac{1}{2}$. At $t = \frac{1}{2}$, $L = \dot{L} = (15/16)^{1/3}$. For $t > \frac{1}{2}$, we set $X = L - Y$ where $Y = \dot{L}$. The surfactant distribution in region I can then be computed, ensuring that Γ and Γ_x are continuous at $x = X$. It is

$$\Gamma = 2Y^2\left(1 - \frac{Y}{3L}\right) + \frac{Y}{2L}(X^2 - x^2), \qquad 0 \leqslant x \leqslant X. \tag{5.8}$$

Some Γ-distributions for values of $t \geqslant \frac{1}{2}$ are shown in figure 5, with bullets separating the viscous region I from the inertial region II. Note that at large times, (5.8) reduces to (5.4) as required. It follows that for $t > \frac{1}{2}$,

$$M_I = \tfrac{1}{3}YL^2\left(1 - \frac{Y}{L}\right)\left(1 + \frac{4Y}{L} - \frac{Y^2}{L^2}\right), \qquad M_{II} = \tfrac{4}{3}Y^3\left(1 - \frac{Y}{5L}\right),$$

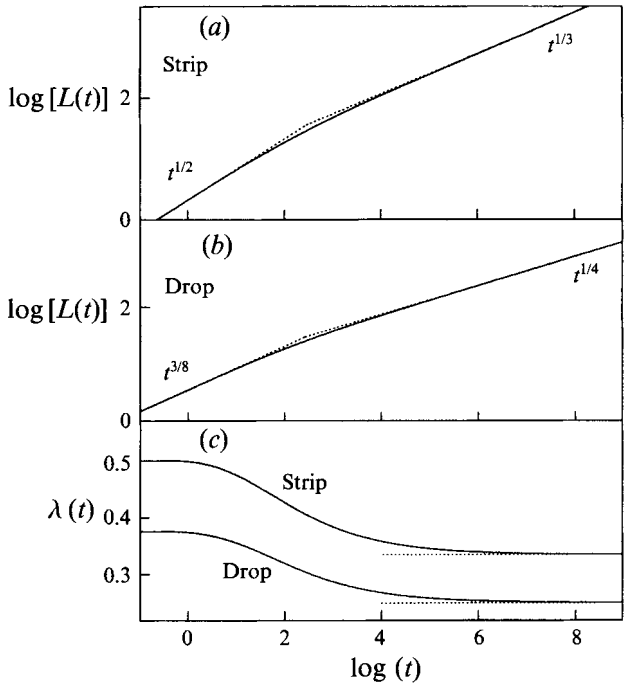

FIGURE 6. The effect of finite depth on spreading rates: the monolayer length $L(t)$ evolves from growing like $t^{1/2}$ to $t^{1/3}$ for a strip (*a*), and from $t^{3/8}$ to $t^{1/4}$ for a drop (*b*); the asymptotes are shown as dotted lines. (*c*) $\lambda = t\dot{L}/L$ as a function of time.

so imposing the condition $M_I + M_{II} = 1$ gives

$$L^3 + 3L^2Y - L\left[Y^2 + \frac{3}{Y}\right] + \tfrac{1}{5}Y^3 = 0. \tag{5.9}$$

The root of (5.9) connecting $L = Y = (15/16)^{1/3}$ with the asymptotic branch $L^2Y \sim 3$ describes the evolution of the monolayer. The corresponding ordinary differential equation for $L(t)$ can be solved numerically; the solution for a strip is shown in figure 6.

The transition between inertia-dominated and viscosity-dominated spreading is best demonstrated by plotting $\lambda = t\dot{L}/L = \mathrm{d}(\log L)/\mathrm{d}(\log t)$ *vs.* time: see figure 6. $\lambda = \frac{1}{2}$ for $0 < t \leqslant \frac{1}{2}$, and then $\lambda(t)$ diminishes smoothly and monotonically to $\frac{1}{3}$. Correspondingly, the inertial region II shrinks (figure 5) and the viscous region I grows, relative to $L(t)$: $Y/L = 0.1$ (0.01) at $t \approx 4.5$ (36.4), when $L \approx 2.85$ (6.62) and $\lambda \approx 0.45$ (0.365). Note that λ remains significantly different from $\frac{1}{3}$ even when $Y/L = 0.01$. The surfactant evolves from a parabolic to a linear distribution at the monolayer's leading edge; there will be a corresponding transition in the film height at this point, from an initially parabolic shape (figure 3*b*) to the abrupt discontinuity predicted by lubrication theory (Borgas & Grotberg 1988). The steeper gradient in the shrinking inertial region makes the monolayer slightly shorter than its asymptotic length at large t, $(9t)^{1/3}$, as is demonstrated in figure 6(*a*). Note that when $L \sim (9t)^{1/3}$, the width of the inertial region $Y = \dot{L} \propto t^{-2/3}$, as predicted by JG.

A similar argument may be used to determine the evolution of a drop. Imposing a mass constraint $\int_0^{L(t)} x\Gamma \,\mathrm{d}x = 1$, rescaling $x = (\mathscr{M}\mathscr{R})^{1/4}\tilde{x}$, $t = \mathscr{R}\tilde{t}$, $\Gamma = (\mathscr{M}/\mathscr{R})^{1/2}\tilde{\Gamma}$ and dropping the tildes, a solution is again sought with velocity distribution $u = \dot{L}x/L$.

Initially,

$$L = \left(\frac{35}{16}\right)^{1/4} \left[\frac{8t}{3}\right]^{3/8}, \qquad 0 < t \leqslant \tfrac{3}{8}.$$

The mass constraint for $t > \frac{3}{8}$ may be shown to be

$$L^4 + 4L^3 Y - 2L^2 Y^2 + 4L\left(\frac{Y^3}{5} - \frac{2}{Y}\right) - \frac{Y^4}{7} = 0.$$

The branch we require connects $L = Y = (35/16)^{1/4}$ to the asymptote $L^3 Y = 8$. The ultimate viscous solution is

$$\Gamma = \left(\frac{1}{2t}\right)^{1/2} - \frac{x^2}{8t}, \qquad 0 < x \leqslant (32t)^{1/4}.$$

Computing the solution numerically, we find that $\lambda = t\dot{L}/L$ diminishes from $\frac{3}{8}$ to $\frac{1}{4}$ at much the same rate as for the strip (figure 6*c*). In both cases, λ falls to within 10% of its ultimate value within a dimensional time $85H_0^2/\nu$, irrespective of the Reynolds number of the original flow (provided, of course, that it is initially large).

6. Discussion

The spreading of a dilute insoluble surfactant monolayer on the free surface of a deep viscous liquid has been considered. Two monolayer configurations of fundamental importance have been examined, a planar strip and an axisymmetric drop, complementing the fixed line-source (planar front) case studied by Foda & Cox (1980). After an initial transient period, solutions approach a self-similar form, in which a strip spreads like $t^{1/2}$ and a drop spreads like $t^{3/8}$. For both distributions, self-similarity requires that the surface velocity $u_s \propto x/t$ along the length of the monolayer (making this an unsteady stretching flow), conveniently decoupling the surfactant transport equation from the flow problem. For sufficiently small monolayers, the effects of gravity are weak enough for the spatial nonuniformity of the velocity field to generate displacements of the free surface (see $H(X)$ in figure 2). The midpoint of a strip, for example, is displaced downwards by a distance that behaves asymptotically like $1.343(\nu t)^{1/2} + C$, where C is a constant arising from an inner layer which must exist at the origin in order for the solution to adjust to the appropriate symmetry boundary condition (§3.1.1). The monolayer's leading edge behaves like a rigid plate; here the free surface is elevated with a characteristic parabolic shape, and the shear stress (given by $-G_X$, figure 2) is singular. The locally large gradients in $H(X)$ may be smoothed by capillary forces; the singularity in the surfactant concentration $G(X)$ may be smoothed by either surface diffusion or by weak concentrations of surfactant on the surface of the undisturbed fluid (§3.2.1). In most cases the corresponding sublayers at the monolayer's leading edge grow quasi-steadily relative to the length of the monolayer, so that each effect may have the capacity to dominate the flow at large times. Surface contamination, for example, ultimately causes disturbances to the fluid to spread like $t^{3/4}$, regardless of the monolayer configuration (§4), and introduces a significant region of longitudinal free-surface compression to the flow (see U_s in figure 4); similarly, if surface diffusion becomes dominant then spreading proceeds like $t^{1/2}$ (JG).

As the monolayer length grows, gravity becomes increasingly important. It acts across the entire flow to suppress the growth of free-surface displacements, by gen-

erating an irrotational flow beneath the boundary layer. Since the strength of the surface-tension gradients driving the basic flow is perpetually diminishing, gravitational effects eventually dominate, so that ultimately the free surface is returned to the horizontal, although at the monolayer's leading edge a weak pressure-driven surface displacement (a 'Reynolds ridge') may be generated (Harper & Dixon 1974; Scott 1982). While gravity competes with the basic flow, spreading is inherently unsteady, losing its self-similar form. However, once the free surface is again horizontal, spreading continues at the same rate as before. The flat-surface flow (figure 3*a*) and the freely deforming surface flow (figure 3*b*) are equivalent, being connected via a Prandtl transformation of the boundary-layer equations (§2.3). In terrestrial situations, gravity is in general more likely to influence the flow than either surface diffusion or capillary forces. It is also likely that, in practice, gravity–capillary waves are generated by whatever experimental mechanism is used to confine the monolayer initially; these waves could significantly interfere with the spreading process.

Of considerable practical interest is the effect of a solid boundary a distance H_0 beneath the free surface. This was examined using a simplified one-dimensional model (in §5) aimed at capturing the dominant time-dependence of the flow. The deep-layer spreading model is appropriate until a time of $O(H_0^2/\nu)$. Thereafter, the flow can be divided into two distinct regions: just upstream of the monolayer's leading edge is an inertial region, in which vorticity is diffusing downwards, uninfluenced by the solid boundary; towards the centre of the monolayer, vorticity has already diffused across the fluid layer, so that vertical gradients in vorticity are gradually eliminated and the flow here is predominantly viscous. As the monolayer spreads, the inertial region shrinks relative to the viscous region, and correspondingly the surfactant distribution evolves from a parabolic to a linear distribution at the monolayer's leading edge (figure 5); meanwhile, the monolayer's spreading rate diminishes, from $t^{1/2}$ to $t^{1/3}$ for a strip, say (figure 6). It is only once the monolayer length greatly exceeds H_0 (i.e. $L \gg 1$ in figure 6) that the residual effects of inertia no longer influence the spreading rate; lubrication theory is then appropriate. Clearly, this heuristic model provides a far from complete description of the flow, but it does establish a strong foundation for future more accurate calculations. These are necessary to explain fully the rupture instability observed experimentally in the very early stages of thin film flows, for example (Gaver & Grotberg 1992), which is a potential hazard in clinical surfactant replacement therapy (JG).

The validity of the deep-layer and finite-depth results presented here should ideally be verified by full numerical solutions of the unsteady boundary-layer (or even Navier–Stokes) equations, allowing the competition between all the different forces to be properly examined. Instabilities of the flow should also be considered: it is possible, for example, that the azimuthal instability of divergent flows, exhibited by Shtern & Hussain (1993) for the Navier–Stokes solutions of Wang (1971) and Bratukhin & Maurin (1967), might be relevant at early times. Further investigations are motivated by the fact that the system can be reduced to a nonlinear diffusion equation, as in §5: a localized monolayer is therefore likely to exhibit 'waiting-time' behaviour, i.e. depending on the initial surfactant distribution, the monolayer boundary may remain stationary for some finite time before it starts to move (Lacey, Ockenden & Tayler 1982). The 'closing-hole' flow demonstrated by Jensen (1994) for a thin film, in which a shrinking clean hole in an otherwise uniform monolayer was shown to be governed by a similarity solution of the second kind with a transcendental exponent, should also be examined in the deep-fluid case.

The $t^{3/4}$ spreading rate for a monolayer fed from a stationary source of constant

surfactant concentration has been verified experimentally by a number of workers since Foda & Cox (1980), including Camp & Berg (1987). If the surfactant source becomes depleted at large times, however, the spreading rate will be reduced and may approach the spreading rates predicted here. Data exhibiting such behaviour have been presented by Joos & Pintens (1977), and by Joos & van Hunsel (1985) who confirmed the $t^{3/4}$ result for a pure surfactant solution, but for a dilute mixture of fluorinated anionic surfactant with a common cationic surfactant they found a spreading exponent of 0.575. This reduced coefficient may well have arisen because of dilution effects, although it equally may be due to a nonlinear equation of state $\sigma(\Gamma)$, for example. Clearly, further experimental studies are called for.

Finally, an important and direct application of the strip solution of §3 is presented. Consider a fixed point source of surfactant held stationary at the free surface of a deep layer of fluid, and suppose that the fluid is moving with a uniform steady current with nondimensional velocity $\mathscr{U}\hat{\boldsymbol{x}}$. Starting at time $t = 0$, the source feeds a monolayer, which is swept downstream by the current: this could represent an oil slick spreading in the surface-tension regime (Hoult 1972) from a stationary tanker, for example. We assume that gravity keeps the free surface horizontal. By seeking a quasi-steady balance between advection by the current in the x-direction, and a transverse spreading in the y-direction due to surface-tension gradients, it is shown in Appendix C that the slick width $Y(x,t)$ is of the form

$$Y \sim \left(\frac{F^2}{\mathscr{U}^5\mathscr{R}}\right)^{1/6} x^{1/2} \tag{6.1}$$

for some function $F(t)$ related to the source strength. The variables here are nondimensionalized following §2. The slick therefore has a quasi-steady self-similar parabolic shape in a particular asymptotic regime, where the leading-order transverse flow is *exactly* the flat-surface strip flow calculated in §3 and shown in figure 3(*a*). This approximation is valid at sufficiently large times over a significant proportion of the slick, far downstream of the source but far upstream of the slick's leading edge (at $x \approx \mathscr{U}t$). The full details of this flow await investigation.

Appendix A. Numerical method

The numerical method used to solve the strip problem (2.25)–(2.27) is briefly described below; the drop problem is very similar. Knowing the structure of the solution at each end of the domain (§§3.1, 3.2), it is convenient to re-express the governing equations in 'natural coordinates', before seeking a numerical solution. Since the stream function $\Phi(X,Y)$ must be of the form $XF(X^2,Y)$ at the origin, and a function of $Y/(1-X)^{1/2}$ at the leading edge, we put $x = X^2$, $y = Y/(1-X^2)^{1/2}$ and

$$\Phi[X,Y] = \tfrac{1}{2}x^{1/2}(1-x)^{1/2}F(x,y), \qquad G(X) = \tfrac{1}{2}(1-x)^{1/2}g(x),$$

$$Q(X) = \tfrac{1}{2}x^{1/2}(1-x)^{1/2}q(x), \qquad H(X) = (1-x)^{1/2}h(x),$$

so that (2.25) becomes

$$x(1-x)\left[F_yF_{xy} - F_xF_{yy} - F_{xy}\right] = F_{yyy} + (1-x)F_y + \tfrac{1}{2}yF_{yy} + (\tfrac{1}{2}-x)FF_{yy} - \tfrac{1}{2}(1-x)F_y^2$$

subject to

$$F = 0, \quad F_y = 1, \quad F_{yy} = 2(1-x)g_x - g \quad \text{on} \quad y = 0, \quad 0 \leqslant x \leqslant 1;$$

$$F \to q(x) \quad \text{as} \quad y \to \infty, \quad \text{where} \quad (\tfrac{1}{2}-x)q + x(1-x)q_x = \tfrac{1}{2}h - x(1-x)h_x.$$

Setting $x = 0$ we recover (3.1) with $F(0, y) = g_0(y)$, with $F_{0yy}(0,0) \approx -0.2086$ and $q(0) = h(0) \approx 1.3422$. At the leading edge, with $x = 1$, we recover the Blasius solution, as in §3.2, with $F_{0yy}(1,0) \approx -0.3316$ and $q(1) = -h(1) \approx 1.7208$.

A numerical solution was obtained using the simple method described by Tuck & Bentwich (1983). The governing equations are parabolic, which means that a solution can be obtained by marching from the leading edge towards the origin. This was done by replacing x-derivatives by first-order backward differences, i.e. $F_x(x, y) \approx [F(x + \Delta x, y) - F(x, y)]/\Delta x$, for some step-length Δx, and then marching from $x = 1$ to $x = 0$. Knowing the solution at $x + \Delta x$, a simple shooting method using a Runge–Kutta routine with Newton iteration is used to determine the solution at x. This was performed at 100 x-stations, with 800 steps in the y-direction, for y values up to 8. In the transformed frame, the solution varies smoothly, and there are no boundary-layer structures to be resolved.

Appendix B. Spreading with contaminant: integral approximation

We seek here T-independent solutions of (4.4)–(4.6). As in §2.4, the surfactant transport equation (4.5) simplifies to an exact derivative for the strip and drop cases. Assuming $G \to 0$ and $U \to 0$ as $X \to \infty$, $U(X,0) = \frac{3}{4}XG(X)$ for n=1, 2. Setting $U(X,Z) = XG(X)F(X,Z)$ for some function F, (4.4) becomes

$$F_{ZZ} + \tfrac{1}{2}ZF_Z + \tfrac{3}{4}XF_X + \tfrac{1}{4}(3n + 4 + 3\phi)F = 0 \quad \text{in} \quad Z \geqslant 0,$$

with $F(X,0) = \frac{3}{4}$, $F_Z(X,0) = \phi/X^2$, $F \to 0$ as $Z \to \infty$. The solution depends on G only through the quantity $\phi(X) \equiv XG_X/G$. Writing $Q = XG(X)q(X)$, (4.7) becomes

$$(2 + 3n + 3\phi)q + 3Xq_X = 4\phi/X^2. \tag{B 1}$$

We now seek an integral approximation by assuming that F takes a specific form, namely $F = \frac{3}{4}e^{-Z/\delta(X)}$. Then, the flow rate $q = \frac{3}{4}\delta$, the tangential stress condition at $Z = 0$ is $3/(4\delta) = -\phi/X^2$ and so $q\phi = -(\frac{3}{4}X)^2$. Substituting for ϕ in (B 1) gives

$$q_X = \frac{-3}{16Xq}\left[(2 + 3n)\left(\frac{4q}{3}\right)^2 - 3X^2q + 4\right] \qquad (n = 1, 2). \tag{B 2}$$

A phase-plane analysis shows that there is a unique solution which satisfies $q \to 0$ as $X \to \infty$, which is that given by the balance $q \sim 4/3X^2$. In this limit $\phi \sim -3^3X^4/4^3$, so at leading order

$$G \sim G_1 \exp\left[-3^3\left(\tfrac{1}{4}X\right)^4\right] \quad \text{as } X \to \infty \tag{B 3}$$

for some constant G_1. As expected, the corresponding solution of (B 2) is singular in the limit $X \to 0$, with the dominant terms here being $q_X = -(2 + 3n)q/(3X)$, so that $q \sim q_0X^{-(n+2/3)}$. Numerical integration of (B 2) shows that $q_0 \approx 1.1816$ for a strip, 1.870 for a drop. Correspondingly,

$$G = G_0 \exp\left[\int_0^X \frac{\phi}{X}\,\mathrm{d}X\right], \quad \text{where} \quad \phi = -\frac{1}{q}\left(\tfrac{3}{4}X\right)^2,$$

approaches a constant G_0 as $X \to 0$, consistent with the anticipated singular behaviour $Q \sim X^{(1/3)-n}$ as $X \to 0$ (§4.1).

$G(X)$ and $Q(X)$ have been computed for a strip, assuming that $G(0) = 1$, and are

shown in figure 4. Since ϕ varies for a strip like X^4 for large X, and $X^{11/3}$ for small X, (B 3) with $G_1 = 1$ is a reasonable approximation of the function over the complete domain; it may also be used to compute a good approximation to $U_s = \frac{3}{4}XG$, as shown in the figure.

Appendix C. A stationary surfactant source in a uniform stream

Consider a stationary surfactant point source at the free surface of a fluid layer which is moving with a uniform, steady current $\mathscr{U}\hat{\mathbf{x}}$: this is equivalent to a source moving with speed $-\mathscr{U}\hat{\mathbf{x}}$ with respect to stationary fluid. The speed $\mathscr{U}$ is nondimensionalized following the scheme in §2. Writing (u, v, w) as the fluid velocity components relative to the moving current, the full governing equations for a monolayer spreading from a stationary source on a clean horizontal free surface, in the absence of surface diffusion, are

$$u_x + \underline{v_y + w_z} = 0,$$
$$u_t + \mathscr{U}u_x + uu_x + vu_y + wu_z = \mathscr{R}^{-1}u_{zz},$$
$$\underline{v_t + \mathscr{U}v_x} + uv_x + \underline{vv_y + wv_z} = \underline{\mathscr{R}^{-1}v_{zz}},$$

with, on $z = 0$,

$$\underline{w = 0}, \quad u_z = \Gamma_x, \quad \underline{v_z = \Gamma_y}, \quad \Gamma_t + \underline{\mathscr{U}\Gamma_x} + (u_s\Gamma)_x + \underline{(v_s\Gamma)_y} = 0$$

and

$$u \to 0, \quad \underline{v \to 0} \quad \text{as} \quad z \to \infty.$$

We seek a quasi-steady balance (represented by the underlined terms, above) between advection by the current in the x-direction, and a transverse spreading in the y-direction due to surface-tension gradients: this balance is analogous to that identified by Smith (1973) in describing the shape of a viscous gravity current moving down an inclined plane (for details see Lister 1992). The reduced surfactant transport equation admits a flux condition

$$\frac{\mathrm{d}}{\mathrm{d}x}\left[\int_{-Y(x,t)}^{Y(x,t)} \mathscr{U}\Gamma \, \mathrm{d}y\right] = 0, \quad \text{i.e.} \quad \int_{-Y(x,t)}^{Y(x,t)} \mathscr{U}\Gamma \, \mathrm{d}y = F(t),$$

where $F(t)$ is related to the unsteady source strength and $Y(x,t)$ represents the slick boundary, i.e. $\Gamma(x, Y, t) = 0$. The reduced governing equations are then completely analogous to those describing a spreading strip on a flat surface (i.e. (2.1), (2.4) and (2.8)), with $x/\mathscr{U}$ effectively a time-like coordinate.

The appropriate scalings for self-similar solutions of the reduced equations are as follows: downward diffusion of vorticity ($\mathscr{U}v_x \sim \mathscr{R}^{-1}v_{zz}$) implies that $z \sim (x/\mathscr{U}\mathscr{R})^{1/2}$; the integral flux condition implies that $\Gamma \sim F/\mathscr{U}y$; the transverse shear-stress condition gives $v \sim \Gamma z/y$; the balance between advection and transverse spreading gives $v \sim Uy/x$ and so mass conservation gives $w \sim (\mathscr{U}/\mathscr{R}x)^{1/2}$; thus (6.1) follows. To determine when this scaling is valid, we must establish the conditions for the remaining terms to be negligible. Noting that $u \sim \Gamma z/x$, $v_t \ll \mathscr{U}v_x$ requires that $x \ll \mathscr{U}t$, while $u \ll \mathscr{U}$ and $u_x \ll v_y$ require that $y \ll x$. Equation (6.1) is therefore applicable far downstream of the near-source region (where $x \sim y$), far upstream of the slick's leading edge (where $x \sim \mathscr{U}t$), and at times sufficiently large (depending on the source strength) for these two zones to be widely separated.

REFERENCES

AHMAD, J. & HANSEN, R. S. 1972 A simple quantitative treatment of the spreading of monolayers on thin liquid films. *J. Colloid Interface Sci.* **38**, 601–604.

BANKS, W. H. H. 1983 Similarity solutions of the boundary-layer equations for a stretching wall. *J. Méc. Théor. Appl.* **2**, 375–392.

BANKS, W. H. H. & KUIKEN, M. B. 1986 Eigensolutions in boundary-layer flow adjacent to a stretching wall. *IMA J. Appl. Maths* **36**, 263–273.

BORGAS, M. S. & GROTBERG, J. B. 1988 Monolayer flow on a thin film. *J. Fluid Mech.* **193**, 151–170.

BRATUKHIN, YU. K. & MAURIN, L. N. 1967 Thermocapillary convection in a fluid filling a half-space. *J. Appl. Math. Mech.* **31**, 577–580 (in Russian).

BUCKMASTER, J. 1973 Viscous-gravity spreading of an oil slick. *J. Fluid Mech.* **59**, 481–491.

CAMP, D. W. & BERG, J. C. 1987 The spreading of oil on water in the surface-tension regime. *J. Fluid Mech.* **184**, 445–462.

CRANE, L. J. 1970 Flow past a stretching plate. *Z. Angew. Math. Phys.* **21**, 645–647.

DAGAN, Z. 1984 Spreading of films of adsorption on a liquid surface. *Physico Chem. Hydrodyn.* **5**, 43–51.

DIPIETRO, N. D. HUH, C. & COX, R. G. 1978 The hydrodynamics of the spreading of one liquid on the surface of another. *J. Fluid Mech.* **84**, 529–549.

ESPINOSA, F. F., SHAPIRO, A. H., FREDBERG, J. J. & KAMM, R. D. 1993 Spreading of a small surfactant bolus on a thin film lining an airway. *J. Appl. Physiol.* **75**, 2028–2039.

FODA, M. & COX, R. G. 1980 The spreading of thin liquid films on a water-air interface. *J. Fluid Mech.* **101**, 33–51.

GAVER, D. P. III & GROTBERG, J. B. 1990 The dynamics of a localized surfactant on a thin film. *J. Fluid Mech.* **213**, 127–148.

GAVER, D. P. III & GROTBERG, J. B. 1992 Droplet spreading on a thin viscous film. *J. Fluid Mech.* **235**, 399–414.

GOLDSTEIN, S. 1965 On backward boundary layers and flow in converging passages. *J. Fluid Mech.* **21**, 33–45.

GROTBERG, J. B. 1994 Pulmonary flow and transport phenomena. *Ann. Rev. Fluid Mech.* **26**, 529–571.

GROTBERG, J. B., HALPERN, D. & JENSEN, O. E. 1995 The interaction of exogenous and endogenous surfactant: spreading-rate effects. *J. Appl. Physiol.* **78**, 750–756.

HARPER, J. F. 1992 The leading edge of an oil slick, soap film, or bubble stagnant cap in Stokes flow. *J. Fluid Mech.* **237**, 23–32.

HARPER, J. F. & DIXON, J. N. 1974 The leading edge of a surface film on contaminated water. *Proc. Fifth Australasian Conf. Hydraulics Fluid Mech., Christchurch, NZ* Vol. 2, pp. 499–505.

HIEMENZ, K. 1911 Die Grenzschicht an einem in den gleichförmigen Flüssigkeitsstrom eingetauchten geraden Kreiszylinder. *Dinglers Polytech. J.* **326**, 321.

HOULT, D. P. 1972 Oil spreading on the sea. *Ann. Rev. Fluid Mech.* **4**, 341–368.

JENSEN, O. E. 1994 Self-similar, surfactant-driven flows. *Phys. Fluids* **6**, 1084–1094.

JENSEN, O. E. & GROTBERG, J. B. 1992 Insoluble surfactant spreading on a thin viscous film: shock evolution and film rupture. *J. Fluid Mech.* **240**, 259–288 (herein called JG).

JOOS, P. & HUNSEL, J. VAN 1985 Spreading of aqueous surfactant solutions on organic liquids. *J. Colloid Interface Sci.* **106**, 161–167.

JOOS, P. & PINTENS, J. 1977 Spreading kinetics of liquids on liquids. *J. Colloid Interface Sci.* **60**, 507–513.

KARKARE, M. V., LA, H. T. & FORT, T. 1993 Criteria for effectiveness of surfactants as water-moving agents in "unsaturated" wet sand. *Langmuir* **9**, 1684–1690.

KUIKEN, H. K. 1981 On boundary layers in fluid mechanics that decay algebraically along stretches of wall that are not vanishingly small. *IMA J. Appl. Maths* **27**, 387–405.

LACEY, A. A., OCKENDEN, J. R. & TAYLER, A. B. 1982 Waiting-time solutions of a nonlinear diffusion equation. *SIAM J. Appl. Maths* **42**, 1252–1264.

LISTER, J. R. 1992 Viscous flows down an inclined plane from point and line sources. *J. Fluid Mech.* **242**, 631–653.

LISTER, J. R. & KERR, R. C. 1989 The propagation of two-dimensional and axisymmetric viscous gravity currents at a fluid interface. *J. Fluid Mech.* **203**, 215–249.

MA, P. K. H. & HUI, W. H. 1990 Similarity solutions of the two-dimensional unsteady boundary-layer equations. *J. Fluid Mech.* **216**, 537–559.

MCCUTCHEN, C. W. 1970 Surface films compacted by moving water: demarcation lines reveal film edges. *Science* **170**, 61–64.

MOCKROS, L. F. & KRONE, R. B. 1968 Hydrodynamics effects on an interfacial film. *Science* **161**, 361–363.

RAJESWARI, V., KUMARI, M. & NATH, G. 1993 Unsteady three-dimensional boundary layer flow due to a stretching surface. *Acta Mechanica* **98**, 123–141.

SCOTT, J. C. 1982 Flow beneath a stagnant film on water: the Reynolds ridge. *J. Fluid Mech.* **116**, 283–296.

SHTERN, V. & HUSSAIN, F. 1993 Azimuthal instability of divergent flows. *J. Fluid Mech.* **256**, 535–560.

SMITH, P. C. 1973 A similarity solution for slow viscous flow down an inclined plane. *J. Fluid Mech.* **58**, 275–288.

SMITH, S. H. 1994 An exact solution of the unsteady Navier-Stokes equations resulting from a stretching surface. *Trans. ASME E: J. Appl. Mech.* **61**, 629–633.

STUART, J. T. 1966 Double boundary layers in oscillatory viscous flow. *J. Fluid Mech.* **24**, 673–687.

SURMA DEVI, C. D., TAKHAR, H. S. & NATH, G. 1986 Unsteady, three-dimensional, boundary-layer flow due to a stretching surface. *Intl J. Heat Mass Transfer* **29**, 1996–1999.

TROIAN, S. M., HERBOLZHEIMER, E. & SAFRAN, S. A. 1990 Model for the fingering instability of spreading surfactant drops. *Phys. Rev. Lett.* A **65**, 333–336.

TUCK, E. O. & BENTWICH, M. 1983 Sliding sheets: lubrication with comparable viscous and inertia forces. *J. Fluid Mech.* **135**, 51–69.

VAN DYKE, M. 1975 *Perturbation Methods In Fluid Mechanics.* Academic Press.

WANG, C. Y. 1971 Effect of spreading of material on the surface of a fluid — an exact solution. *Intl. J. Nonlin. Mech.* **6**, 255–262.

WANG, C. Y. 1984 The three-dimensional flow due to a stretching flat surface. *Phys. Fluids* **27**, 1915–1917.